



## D3.2

### Report on antenna designs

<b>Project number:</b>	610436
<b>Project acronym:</b>	MATTHEW
<b>Project title:</b>	MATTHEW: Multi-entity-security using active Transmission Technology for improved Handling of Exportable security credentials Without privacy restrictions
<b>Start date of the project:</b>	1 <sup>st</sup> November, 2013
<b>Duration:</b>	36 months
<b>Programme:</b>	FP7-ICT-2013-10

<b>Deliverable type:</b>	Report
<b>Deliverable reference number:</b>	ICT-610436 / D3.2 / 1.1
<b>Activity and Work package contributing to the deliverable:</b>	WP 3
<b>Due date:</b>	June 2015 – M20
<b>Actual submission date:</b>	June 26 <sup>th</sup> , 2015

<b>Responsible organisation:</b>	IFAG
<b>Editor:</b>	Frank Scherber (IFAT), Giuliano Manzi (AMS)
<b>Dissemination level:</b>	Public
<b>Revision:</b>	1.1

<b>Abstract:</b>	This document reports simulation results of three different antenna design concepts selected as possible candidates for implementation in $\mu$ SD and nanoSIM cards. Goal of the document is to highlight advantages and disadvantages of each solution by mean of a comparative analysis of radiated field, required current and achievable load modulation. Furthermore, the document includes recommendations for system design in
------------------	--

	order to minimize radiated emission from active transmission technology based systems, as well as emission test and measurements results of an engineering test active transmitter.
<b>Keywords:</b>	MATTHEW, active transmission technology, antenna simulation, load modulation, radiated emission



This project has received funding from the European Union's Seventh Framework Programme for research, technological development and demonstration under grant agreement n° 610436.

### **Editors**

Frank Scherber (IFAT)

Giuliano Manzi (AMS)

### **Contributors** (ordered according to beneficiary numbers)

Josef Gruber, Frank Scherber (IFAT)

Gregory Capomaggio (GTO)

Giuliano Manzi (AMS)

Erich Wenger (IAIK) – Technical Review

Jens Pohl (IFAG)

### **Disclaimer**

The information in this document is provided “as is”, and no guarantee or warranty is given that the information is fit for any particular purpose. The user uses the information at its sole risk and liability.

## Executive Summary

This deliverable D3.2 “Report on antenna designs” is the second technical deliverable of the work package WP3 “Component Hardware Development”. Together with deliverable D3.1 “Report on active transmission technology” it builds the basis for milestone MS3 “Component hardware ready” and will be continued by the tasks of WP5 “Integration, Prototyping”.

In the last 10 years, contactless technology has been getting more and more interest in the smart card industry and has moved from a very proprietary piece of technology to a more and more standardized technology with ISO/IEC14443 and Near Field Technology (NFC). With NFC, this technology has also moved out of the pure smart card world, going into a variety of form factors and different types of devices.

The key problem though faced by industrial actors has been the constraints the core foundation of contactless smart card relies on: magnetic field coupling. Key constraints have therefore been the need to have big antennas that limit miniaturization and to avoid conducting materials, which basically ‘sink’ the magnetic field. In the last 2 to 3 years, a new piece of technology called active transmission or active load modulation (ALM) has been coming to market addressing some of the limitations of traditional RFID, especially the limitation on the size of the antenna.

This report, assuming that basic principles of active transmission technology are well known, will focus on the analysis of 3 different miniaturized antenna (coil) configurations suitable for integration in very small devices (secure systems) like  $\mu$ SD or nanoSIM cards.

# Contents

<b>Chapter 1</b>	<b>Introduction</b>	<b>1</b>
<b>Chapter 2</b>	<b>Antenna Concepts</b>	<b>2</b>
2.1	Benchmark Model	2
2.1.1	Mechanical	2
2.1.2	Electrical	3
2.2	$\mu$ SD Implementation	4
2.2.1	Antenna Configuration 1 (Planar)	4
2.2.1.1	<i>Description</i>	4
2.2.1.2	<i>Matching Network and Current Consumption</i>	4
2.2.1.3	<i>Radiated Field</i>	6
2.2.1.4	<i>Radiated Field in Presence of Ferrite</i>	7
2.2.2	Antenna Configuration 2 (Solenoid)	9
2.2.2.1	<i>Description</i>	9
2.2.2.2	<i>Matching Network and Current Consumption</i>	10
2.2.2.3	<i>Radiated Field</i>	11
2.2.3	Antenna Configuration 3 (Hybrid)	12
2.2.3.1	<i>Description</i>	12
2.2.3.2	<i>Matching Network and Current Consumption</i>	13
2.2.3.3	<i>Radiated Field</i>	14
2.2.4	Comparison Between all Three Configurations	15
2.2.4.1	<i>Magnetic Field Evaluation in Space and along Defined Directions</i>	15
2.2.4.1.1	2D Plot of Hz and Hx Field Components	15
2.2.4.2	<i> H  Field Planar Plot</i>	16
2.2.4.2.1	Planar Coil	17
2.2.4.2.2	Solenoid	19
2.2.4.2.3	Hybrid	21
2.3	nanoSIM Implementation	23
2.3.1	Antenna Concept	23
2.3.1.1	<i>nanoSIM Antenna Design</i>	23
2.3.2	Antenna Simulation	24
2.3.2.1	<i>Equivalent Antenna Parameter EQV</i>	24
2.3.3	Antenna Matching	25
2.3.3.1	<i>Simulation within Mobile Phone Model</i>	26
2.3.3.2	<i>Radiated Field</i>	27
2.3.4	Conclusion of nanoSIM Simulation	28

2.4	Wearable Devices.....	29
<b>Chapter 3</b>	<b>Load Modulation Simulation .....</b>	<b>31</b>
3.1	Overview of ISO10373-6 Test Specification (for Passive Devices).....	31
3.2	ISO 10373-6 Test Set-up Simulation Model (Class 1).....	33
3.3	Simulation of Solenoid Coil .....	34
<b>Chapter 4</b>	<b>Design Recommendations .....</b>	<b>36</b>
4.1	RF Sub-System Block Diagram.....	36
4.1.1	EMC Mitigation Techniques .....	37
4.2	Example of a Test System (Emission Measurement) .....	38
<b>Chapter 5</b>	<b>Conclusion .....</b>	<b>39</b>
<b>Chapter 6</b>	<b>List of Abbreviations .....</b>	<b>40</b>

## List of Figures

Figure 1: Benchmark model .....	2
Figure 2: Calculation paths .....	3
Figure 3: Matching block diagram .....	3
Figure 4: Planar antenna in $\mu$ SD card format .....	4
Figure 5: Matching network .....	5
Figure 6: System impedance .....	5
Figure 7: Calculated current for planar coil system in $\mu$ SD card format .....	5
Figure 8: Plot direction .....	6
Figure 9: Detailed view of coil in $\mu$ SD socket .....	6
Figure 10: Hz field component along defined directions .....	7
Figure 11: Detailed view of coil in $\mu$ SD socket with ferrite layer .....	7
Figure 12: Hz field component along defined directions (with additional ferrite layer below the coil). .....	8
Figure 13: “Solenoid” antenna in $\mu$ SD card format .....	9
Figure 14: Solenoid based system impedance .....	10
Figure 15: Calculated current for solenoid coil system in $\mu$ SD card format .....	10
Figure 16: Main H field components along defined directions .....	11
Figure 17: 3D detailed view of the solenoid coil .....	11
Figure 18: Hybrid antenna in $\mu$ SD card format .....	12
Figure 19: Hybrid coil matched impedance in $\mu$ SD card format .....	13
Figure 20: Calculated current for hybrid coil system in $\mu$ SD card format .....	13
Figure 21: Relevant Hz, Hx and Hy field components along defined directions .....	14
Figure 22: 3D detailed view of the hybrid coil .....	14
Figure 23: Hz field along V .....	15
Figure 24: Hz field along D .....	15
Figure 25: Hz field along H .....	16
Figure 26: Planar coil  H  field distribution .....	17
Figure 27: Planar coil  Hz  field distribution .....	17
Figure 28: Planar coil  Hy  field distribution .....	18
Figure 29: Planar coil  Hx  field distribution .....	18
Figure 30: Solenoid  H  field distribution .....	19
Figure 31: Solenoid  Hz  field distribution .....	19
Figure 32: Solenoid  Hy  field distribution .....	20
Figure 33: Solenoid  Hx  field distribution .....	20

Figure 34: Hybrid  H  field distribution .....	21
Figure 35: Hybrid  Hz  field distribution.....	21
Figure 36: Hybrid  Hy  field distribution .....	22
Figure 37: Hybrid  Hx  field distribution.....	22
Figure 38: nanoSIM antenna design with ferrite core .....	23
Figure 39: nanoSIM equivalent circuit of an antenna .....	24
Figure 40: ANSYS HFSS EQV antenna simulation .....	24
Figure 41: nanoSIM antenna matching circuit .....	25
Figure 42: nanoSIM design with integrated antenna and contact pads .....	26
Figure 43: Simulation nanoSIM within mobile phone model.....	26
Figure 44: Field plot at the gap.....	27
Figure 45: Field plot at the mid of the model.....	27
Figure 46: Field plot cross the model .....	28
Figure 47: ISO 10373-6 (test set-up view) .....	31
Figure 48: ISO 10373-6 (test set-up view) .....	32
Figure 49: ISO 10373-6 (test set-up view) .....	32
Figure 50: ISO 10373-6 (3D view simulation model).....	33
Figure 51: ISO 10373-6 (circuital model used in co-simulation) .....	33
Figure 52: Output voltage at RFO pins of the IC.....	34
Figure 53: Output current at RFO pins of the IC.....	34
Figure 54: Achieved load modulation .....	35
Figure 55: Power supply filtering .....	36
Figure 56: Matching block diagram.....	36
Figure 57: Mobile device in semi-anechoic chamber.....	38
Figure 58: Radiated emission (black dot) .....	38



## Chapter 1 Introduction

This report will focus on the design of antennas optimized for small form factors like  $\mu$ SD or nanoSIM. Supported by electromagnetic field simulation tools the designs have been developed to overcome the limitations of the metallic environment in a mobile phone like the metal socket or the battery. The simulation models of  $\mu$ SD and nanoSIM sockets consider sockets with a big portion of metallic influence to the  $\mu$ SD card or nanoSIM and sockets with minor metallic influence.

In chapter 2 different antenna coil concepts will be presented and described in more detail together with a benchmark model that emulates a mobile device. The model is needed in order to allow a proper comparison of the different concepts. Outcome is to estimate the radiated field of each configuration and according to it, select the coil that allows better coverage of the area surrounding the mobile device and may guarantee best user experience.

Together with the radiated field the system impedance will be analysed and the matching will be optimized in order to guarantee that each configuration will have the same power consumption allowing a one to one comparison of the radiated field in terms of magnetic field strength as function of distance and field component.

Finally, in chapter 3 by means of simulations the maximum achievable load modulation from the best suited configuration according to ISO 10373-6 test specification will be analysed.

Beside this, in the last chapter basic recommendations needed to avoid spurious emission of active transmission technology based NFC systems will be given together with an overview of FCC emission tests of an engineering active transmission technology transmitter IC.

## Chapter 2 Antenna Concepts

In this section of the report the three main antenna concepts will be investigated. All three concepts will be suitable for integration on SIM,  $\mu$ SIM,  $\mu$ SD and nanoSIM.

The different antenna concepts have been defined with the aim to have a dominant component of the magnetic field in different directions: orthogonal to the mobile device plane for the planar structure, parallel and diagonal to the mobile plane for the solenoid and diagonal for the hybrid configuration.

### 2.1 Benchmark Model

#### 2.1.1 Mechanical

In order to obtain comparable results we have carefully defined a simulation model that emulates in a simplified way a mobile device and a  $\mu$ SD and nanoSIM socket.

The model consists of a planar conductive structure having a size of 140 mm x 70 mm (corresponding to the size of a typical 5" mobile device). The SD/SIM socket has been placed in the middle of the structure to emulate a worst condition configuration (area below the coil structure is fully metalized). Normally the SD/SIM connections are placed on the side of the mobile device with at least on side of the card facing free air condition (absence of metal or loose parts).

An overview of the model showing the metal plane and the card socket is depicted in Figure 1 and an overview of calculation paths in Figure 2.

The field will be plotted for all the investigated cases in 4 main directions: V (orthogonal to the mobile device ref metal plane); H1 and H2 (coplanar to the mobile device ref metal plane); D (along a curve having an angle of  $45^\circ$  with ref plane in the direction of H1). Additionally, for the Hybrid coil configuration the H field will be evaluated also along an additional path D1. Calculation paths are shown in Figure 2.

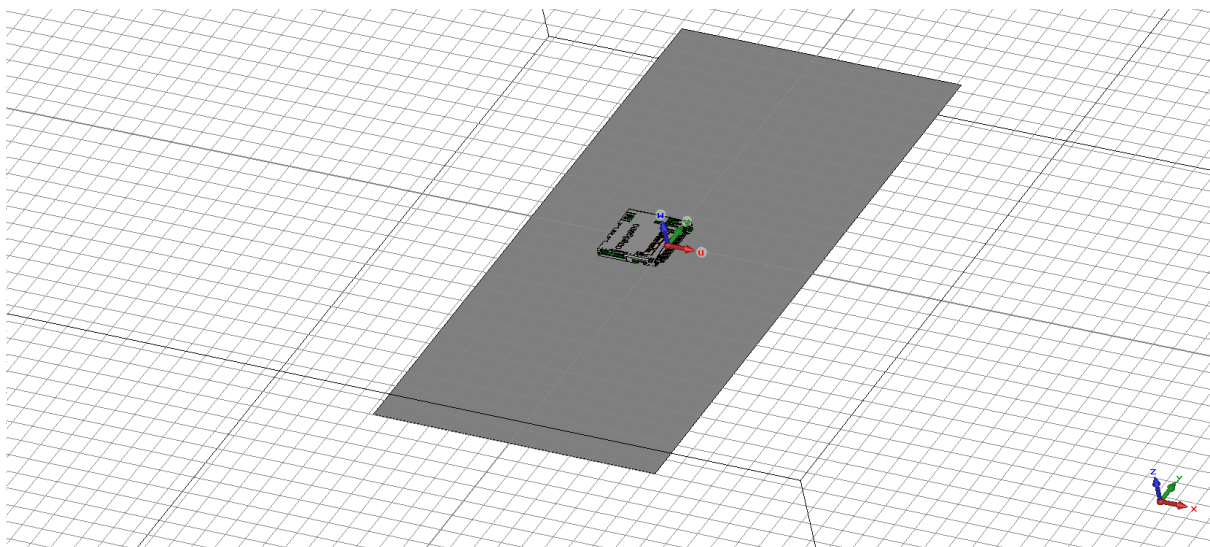


Figure 1: Benchmark model

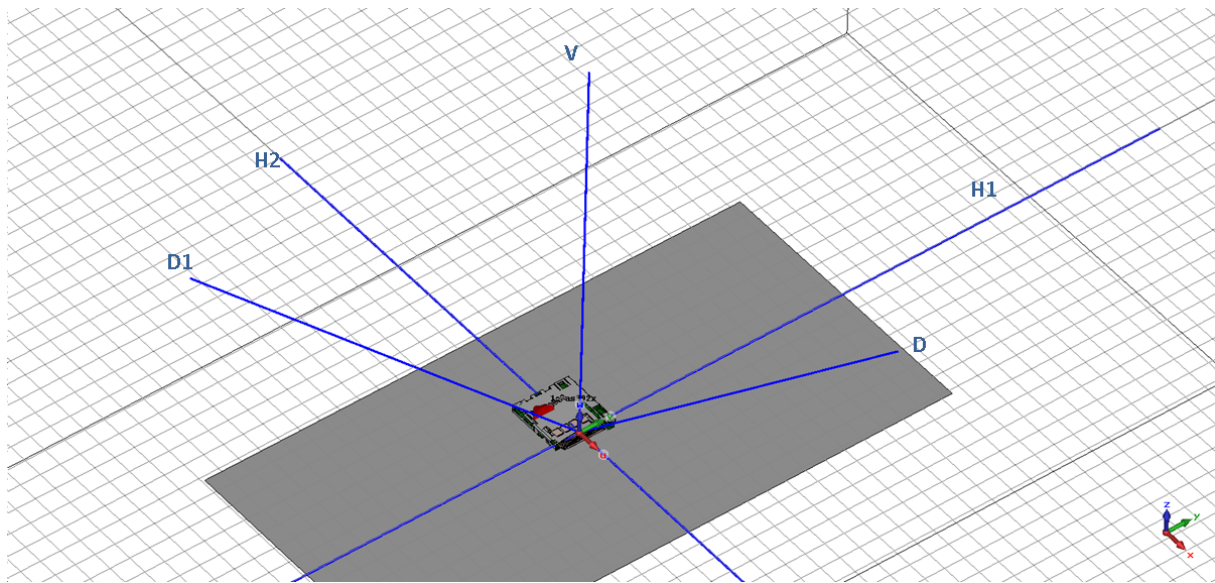


Figure 2: Calculation paths

### 2.1.2 Electrical

Together with the mechanical parameters it is also critical (essential) to define all relevant electrical parameters that will play a major role in the radiated magnetic field.

The main parameter that needs to be controlled in each different design, in order to allow proper comparison between the different coil geometries, is the current flowing in the coil.

The currents flowing into each coil, together with the system driven current, need to be kept similar between all different geometries. This will ensure that each of the geometries will be driven with the same amount of current and will allow direct comparison between all radiated field calculations.

The current is controlled by implementing an ad-hoc matching for each coil configuration. The target impedance that allows maintaining current output levels of about 250mA for each configuration is  $\sim 12 \text{ Ohm}$ . This will allow keeping the power consumption at the same level between all different coil designs.

The matching network implemented in the system can be summarized as cascade of 2 blocks: a low pass filter structure (that has also EMC function, see Chapter 4) and a  $\pi$ -network. The two blocks overlap each other (share one component in order to save in the bill of material). A high level block diagram of the matching is shown in Figure 3.



Figure 3: Matching block diagram

## 2.2 $\mu$ SD Implementation

In this section based on the  $\mu$ SD form factor three different antenna coil concepts will be evaluated and compared with respect to their performance.

### 2.2.1 Antenna Configuration 1 (Planar)

#### 2.2.1.1 Description

The first geometry analysed is a state of the art spiral coil designed as a planar structure. The coil is realized as a rectangular spiral in 8 turns placed over a dielectric substrate area of 10 mm x 3 mm (30 square mm). Outline of the  $\mu$ SD with the coil on the right side (yellow traces) is shown in Figure 4.

The planar coil is intended to generate a strong component of the magnetic field (Hz) along a path orthogonal to the mobile device. However, due to close proximity to the metal plane (representing the mobile device electronics) orthogonal to the magnetic field, together with a possible metal layer on top of the spiral (represented by a possible agnostic configuration of the card socket) may present an high level of noise and do not result in an optimal choice for the final application.



Figure 4: Planar antenna in  $\mu$ SD card format

#### 2.2.1.2 Matching Network and Current Consumption

In order to achieve a realistic calculation of the radiated field the matching network has been tuned in a way that IC output pins (RFO1 and RFO2 in Figure 5) will see an equivalent differential impedance of about  $12\Omega$  as shown in Figure 6. This allows operating the system with an IC output current of about 250mA (Figure 7). The current flowing in the coil is a bit higher due to matching network resonance.

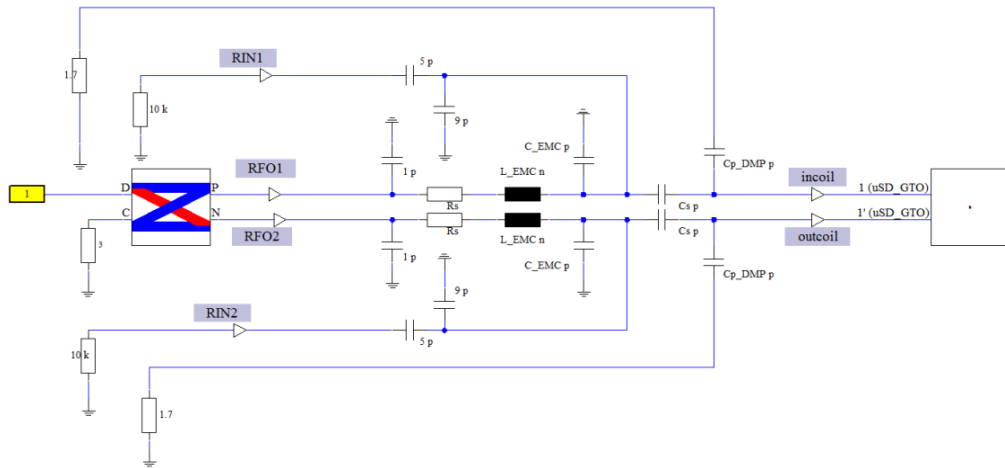


Figure 5: Matching network

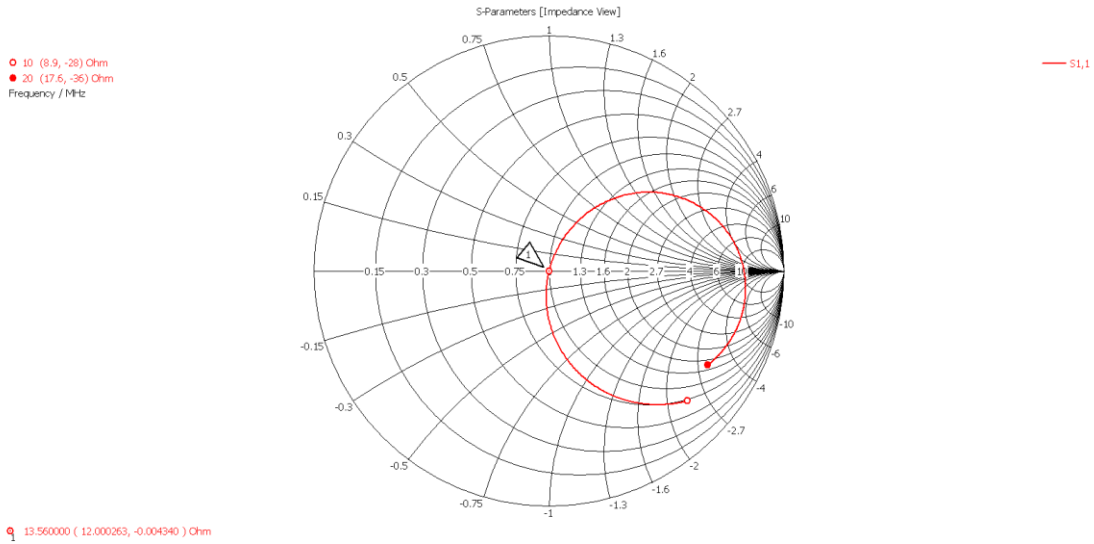


Figure 6: System impedance

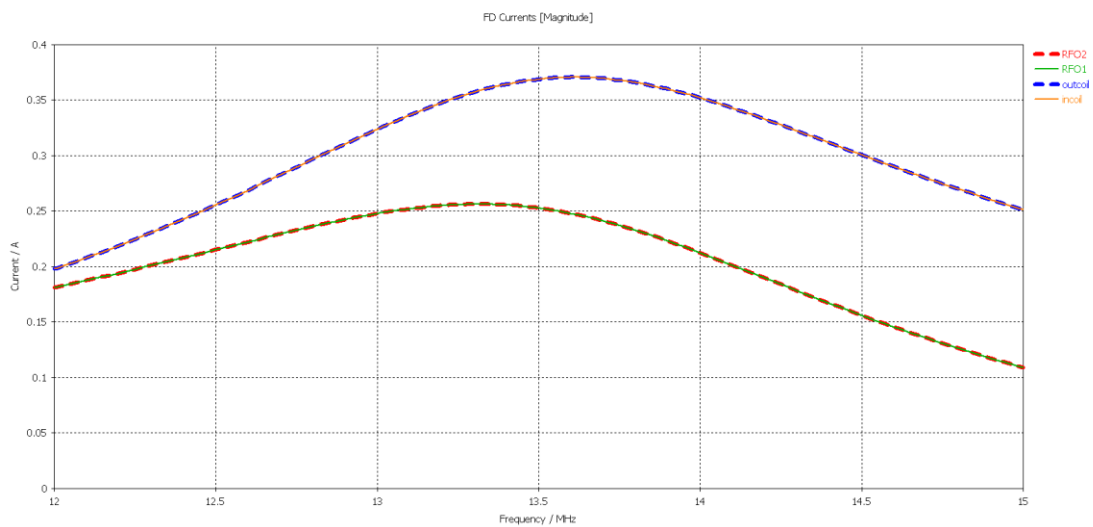


Figure 7: Calculated current for planar coil system in  $\mu$ SD card format

### 2.2.1.3 Radiated Field

The radiated field for the planar rectangular spiral geometry is calculated along paths in Figure 8.

A detailed 3-dimensional view of the planar rectangular spiral coil is shown in Figure 9.

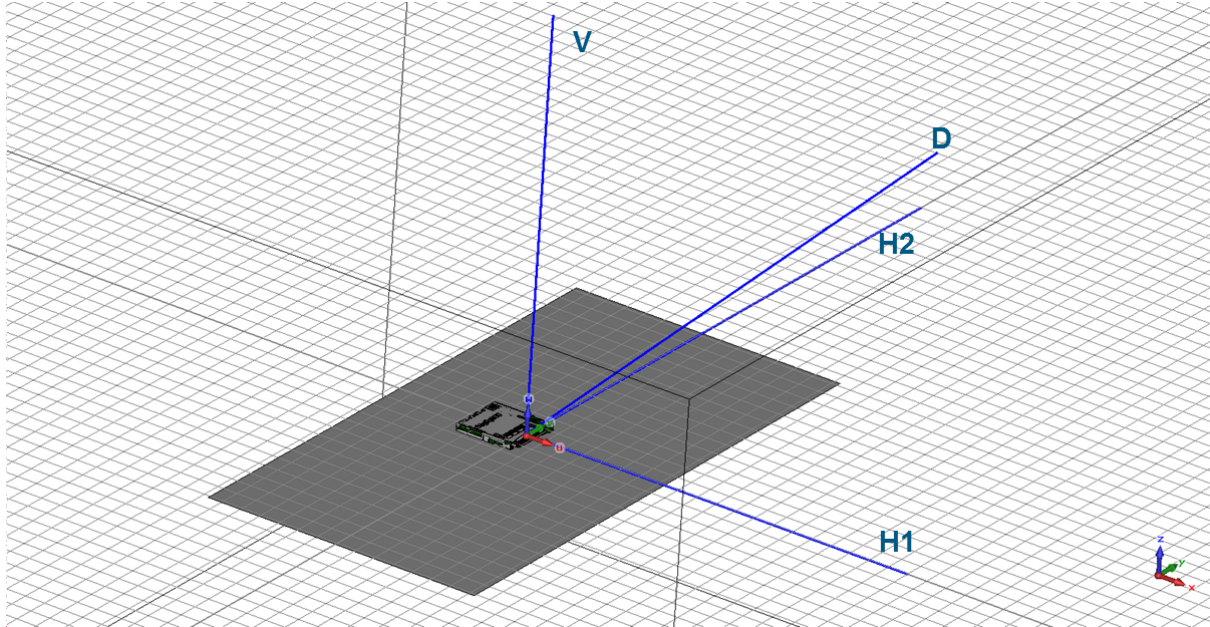


Figure 8: Plot direction

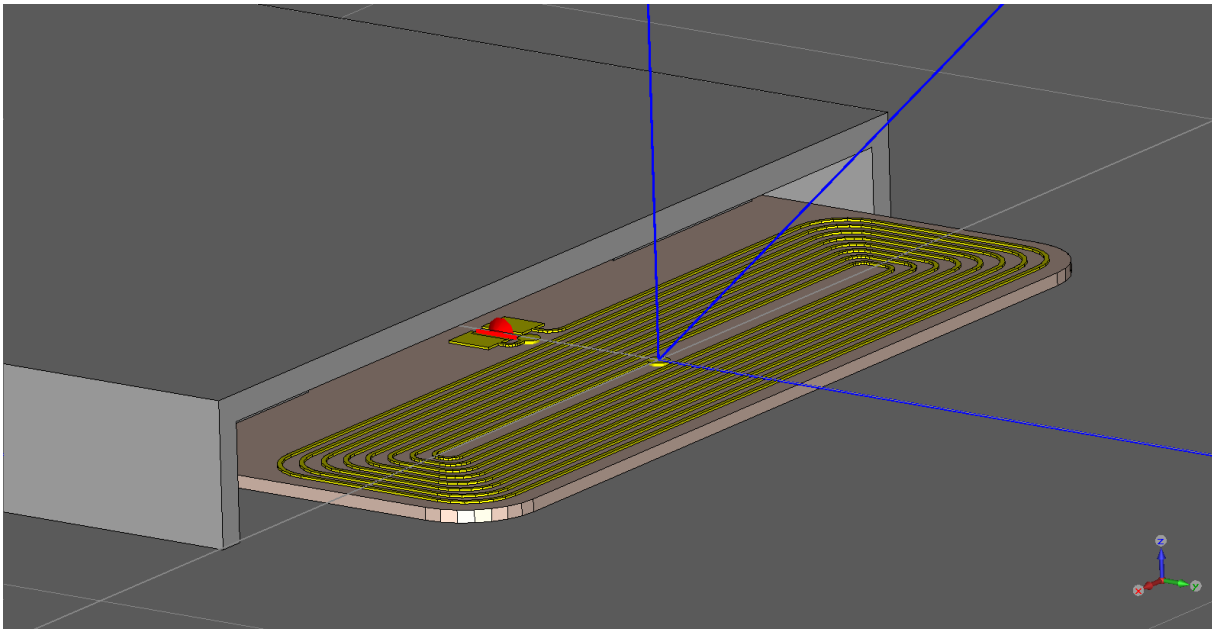


Figure 9: Detailed view of coil in  $\mu$ SD socket

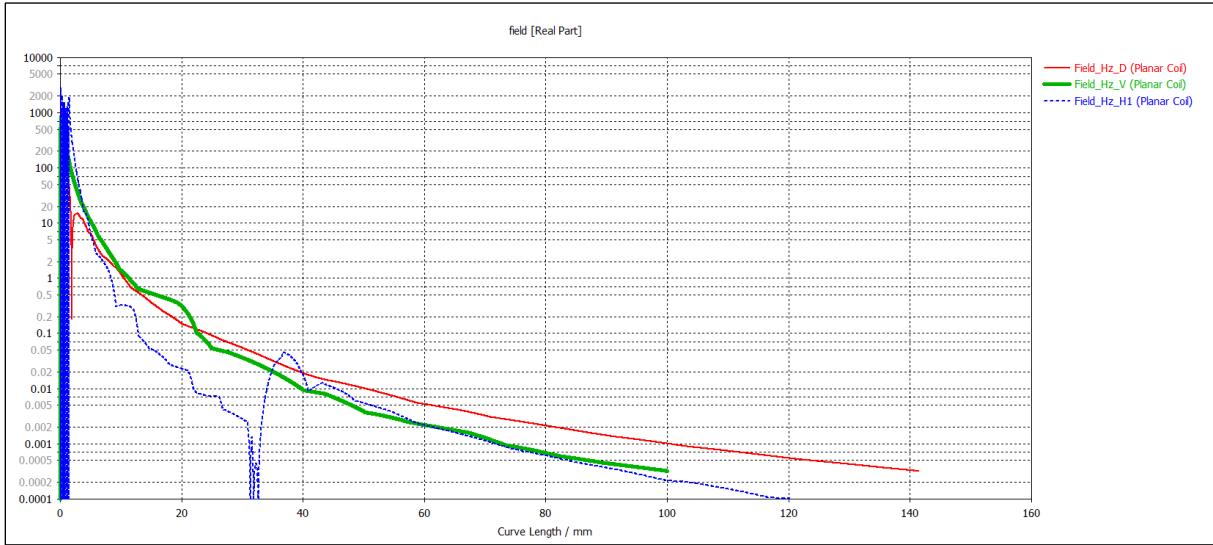


Figure 10: Hz field component along defined directions

From Figure 10 it can be observed that the planar coil generates a dominant Hz field component in the near region (<2 cm from the coil) along the path orthogonal to the mobile device (path V) and after 2 cm the component along D becomes higher than the one along V. Please note the effect on the edge of the mobile device (at ~3.5cm from the coil) the jump on the Hz field component along H1. The jump is due to the end of metallization, it results in a local peak of the magnetic field exactly on the border of the mobile device.

**2.2.1.4 Radiated Field in Presence of Ferrite**

In order to improve the performance of the planar coil configuration a further simulation including a ferrite layer below the coil (in the direction of the metal structure of the mobile device to reduce losses introduced by metal proximity) has been done. Figure 11 shows a structure with a ferrite layer placed below the planar coil’s substrate.

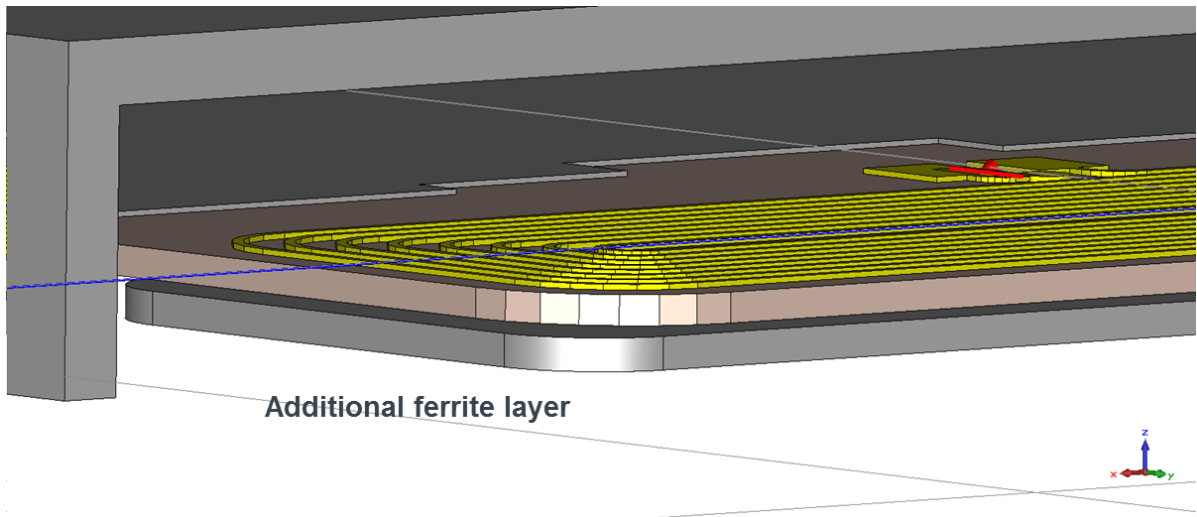


Figure 11: Detailed view of coil in μSD socket with ferrite layer

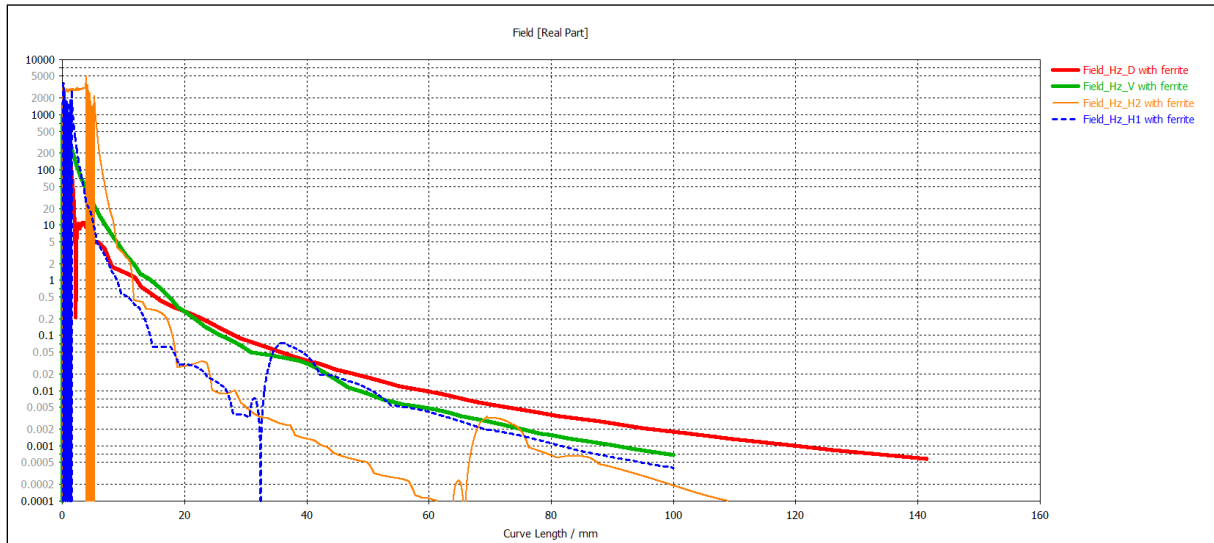


Figure 12: Hz field component along defined directions (with additional ferrite layer below the coil)

From Figure 12 it can be observed that the usage of a ferrite results in a small increase of the level of the radiated Hz field component. This is due to the effect of ferrite to mitigate the losses introduced by the metal plane in the area below the coil. A bigger ferrite layer extending all along the mobile device will be very effective and minimizes losses. Unfortunately this is not applicable and we can only consider a ferrite layer implemented inside the  $\mu$ SD or nanoSIM.



## 2.2.2 Antenna Configuration 2 (Solenoid)

### 2.2.2.1 Description

The second geometry analysed is an innovative solenoid structure having the coil axis parallel to the mobile device metal plane and has a ferrite core. The solenoid structure has a rectangular cross section of 0.45 mm x 1.55 mm and consists of 18 turns (see yellow traces in Figure 13).

The solenoid concept has been designed in order to achieve a dominant component of the magnetic field parallel to the mobile device metal plane (along path H1) as well as a strong field level along the path D.

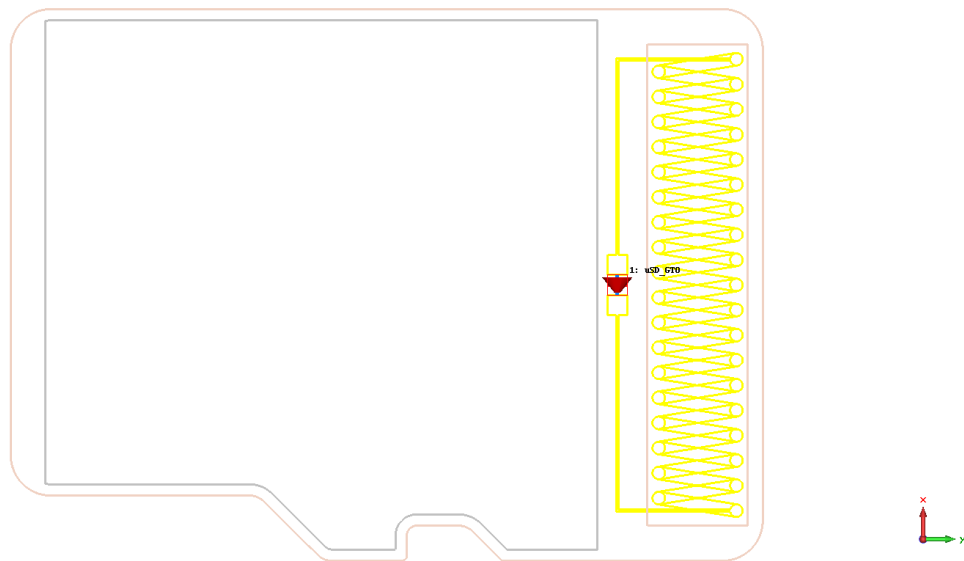


Figure 13: “Solenoid” antenna in  $\mu$ SD card format

### 2.2.2.2 Matching Network and Current Consumption

The matching network configuration has the same configuration as defined in general section 2.1.2 and consists of an EMC filter plus a matching network. The matching as in previous case (planar coil) has been optimized to achieve an impedance of  $12\Omega$  and an output current of  $\sim 250\text{mA}$ . Impedance and calculated currents are shown in Figure 14 and Figure 15, respectively.

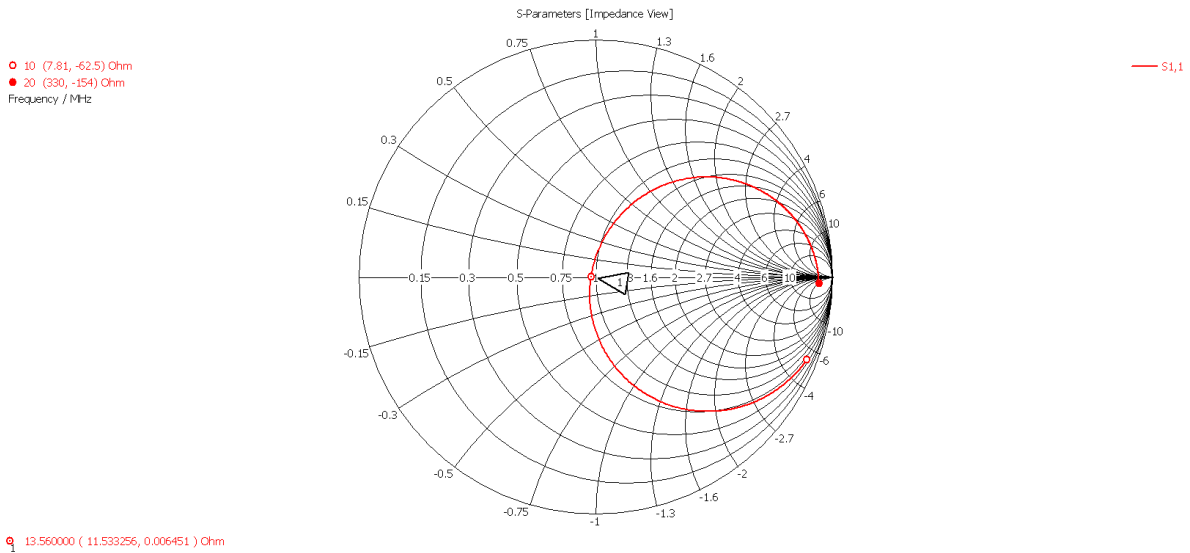


Figure 14: Solenoid based system impedance

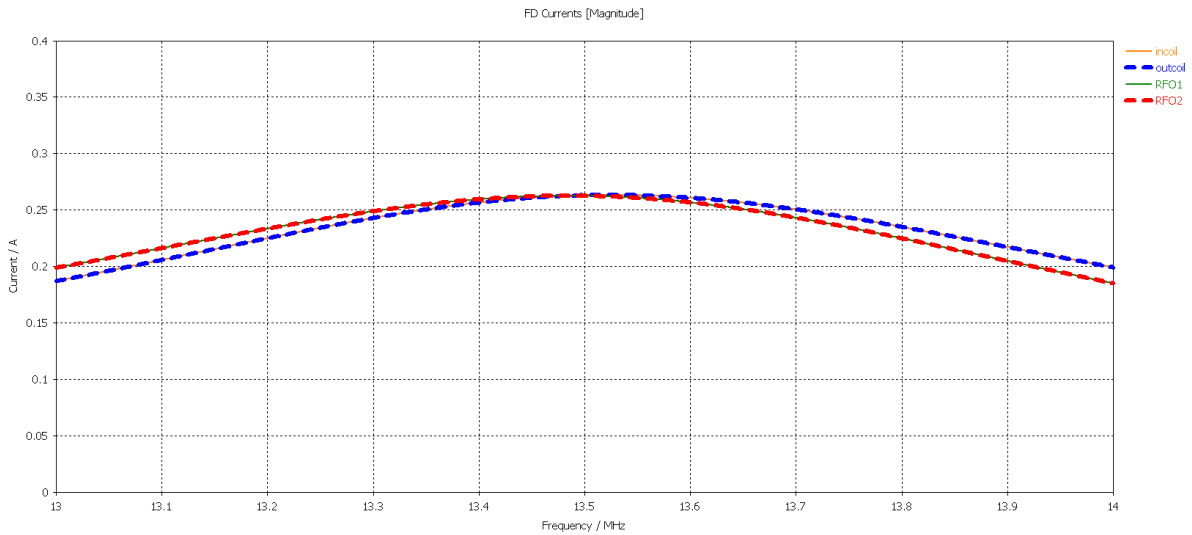


Figure 15: Calculated current for solenoid coil system in  $\mu\text{SD}$  card format

### 2.2.2.3 Radiated Field

The radiated field for the solenoid structure is calculated along paths in Figure 16.

A detailed 3-dimensional view of the solenoid coil structure is shown in Figure 17.

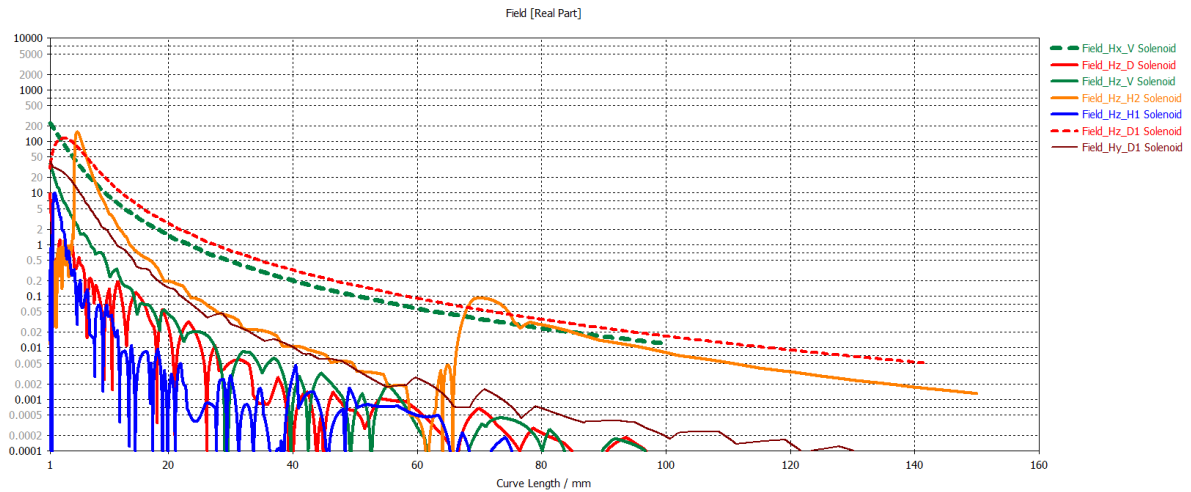


Figure 16: Main H field components along defined directions

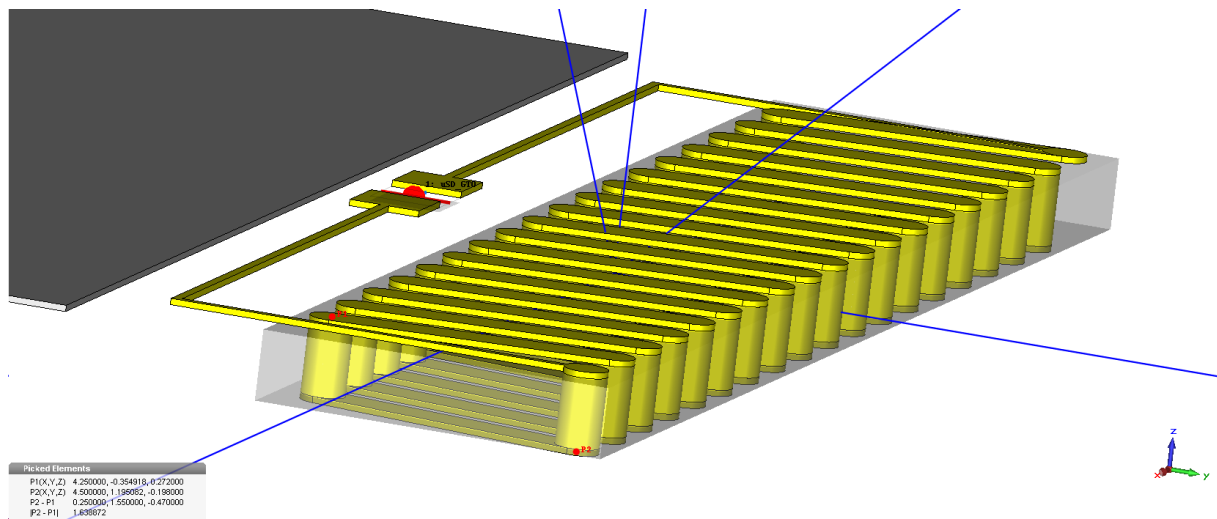


Figure 17: 3D detailed view of the solenoid coil

## 2.2.3 Antenna Configuration 3 (Hybrid)

### 2.2.3.1 Description

The third geometry analysed is an innovative hybrid structure that combines in a single structure a solenoid and a planar coil with the aim to achieve a strong magnetic field along the D paths. The hybrid structure requires an area of 9.6 mm x 2 mm. The rectangular cross section of the solenoid part is 0.45 mm x 1.5 mm and consists of 16 turns (see yellow traces in Figure 18), whereas the planar structure is made of 4 turns.

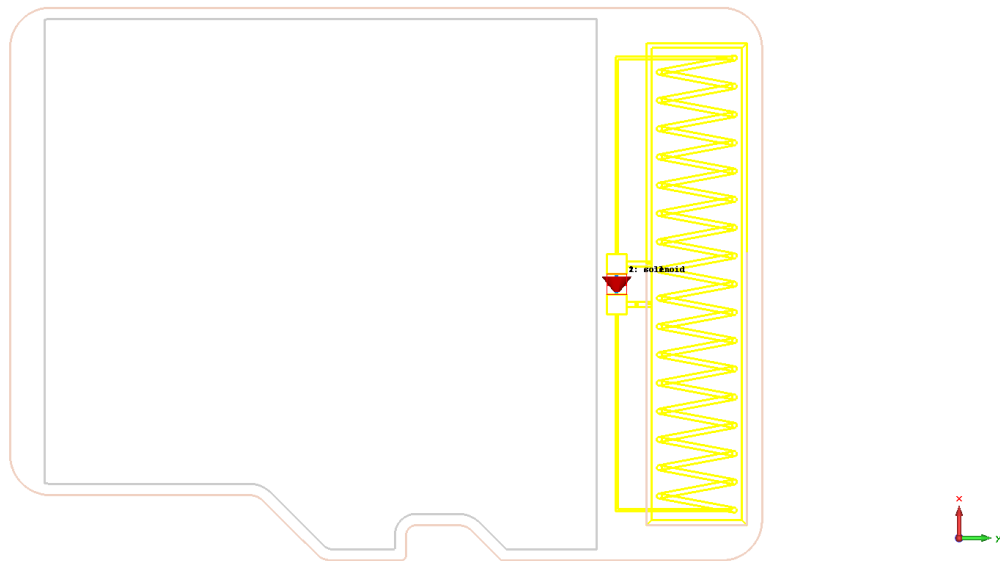


Figure 18: Hybrid antenna in  $\mu$ SD card format

### 2.2.3.2 Matching Network and Current Consumption

The matching network configuration has the same configuration as defined in general section 2.1.2 and consists of an EMC filter plus a matching network. The matching has been optimized to achieve an impedance of  $12\Omega$  and an output current of  $\sim 250\text{mA}$  as in previous two cases (planar coil and solenoid). Impedance and calculated currents are shown in Figure 19 and Figure 20, respectively.

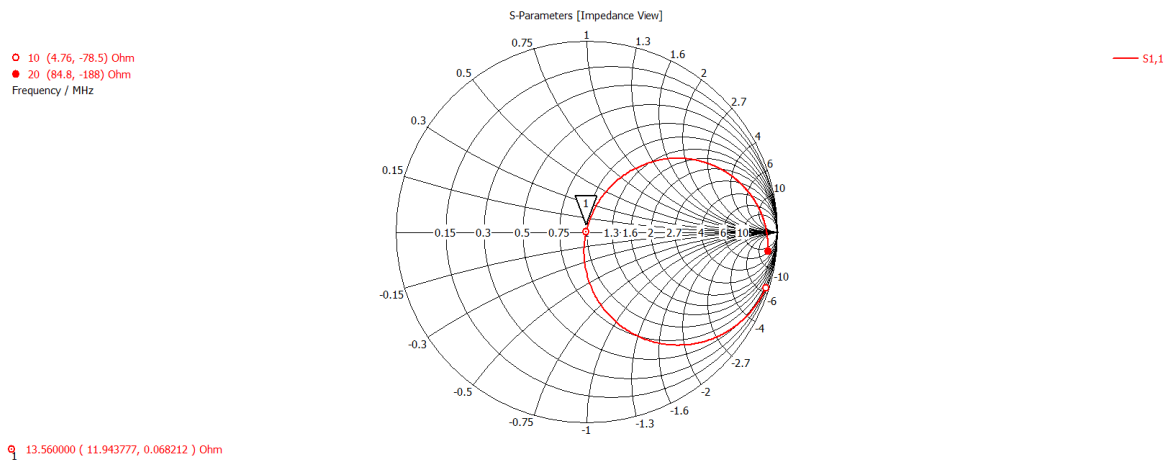


Figure 19: Hybrid coil matched impedance in  $\mu\text{SD}$  card format

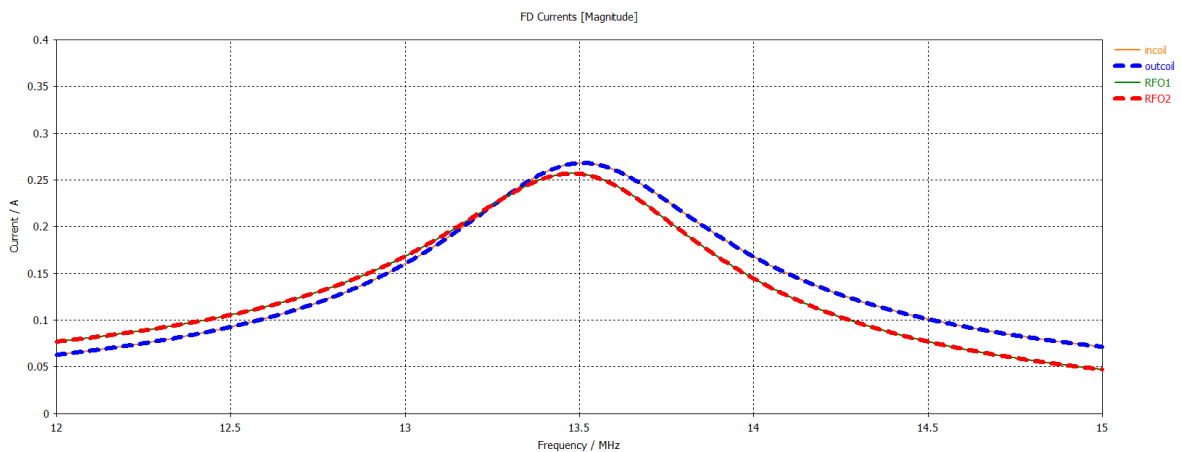


Figure 20: Calculated current for hybrid coil system in  $\mu\text{SD}$  card format

### 2.2.3.3 Radiated Field

The radiated field for the hybrid structure is calculated along paths in Figure 21.

A detailed 3-dimensional view of the hybrid coil structure is shown in Figure 22.

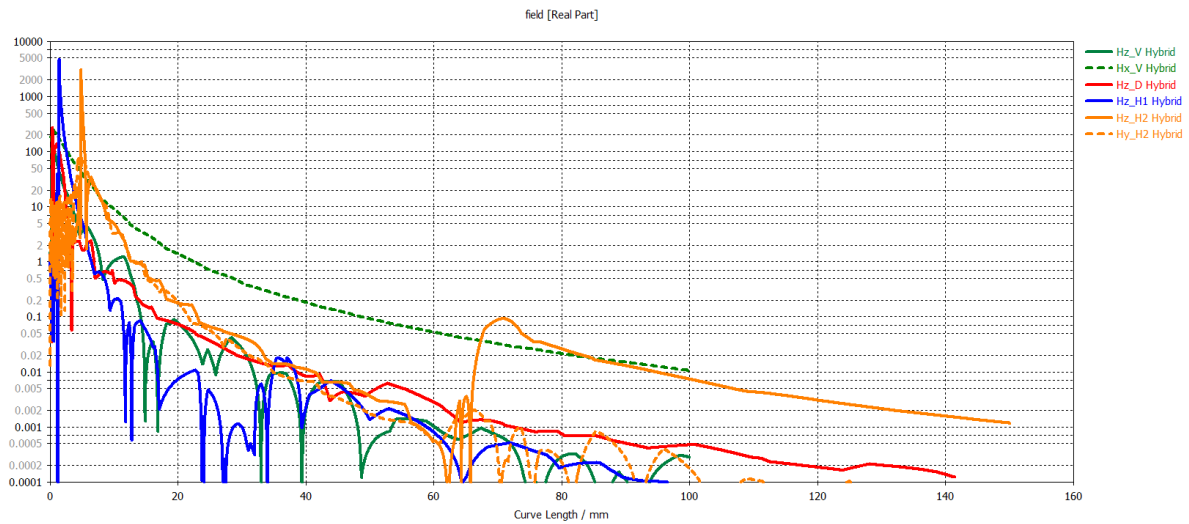


Figure 21: Relevant Hz, Hx and Hy field components along defined directions

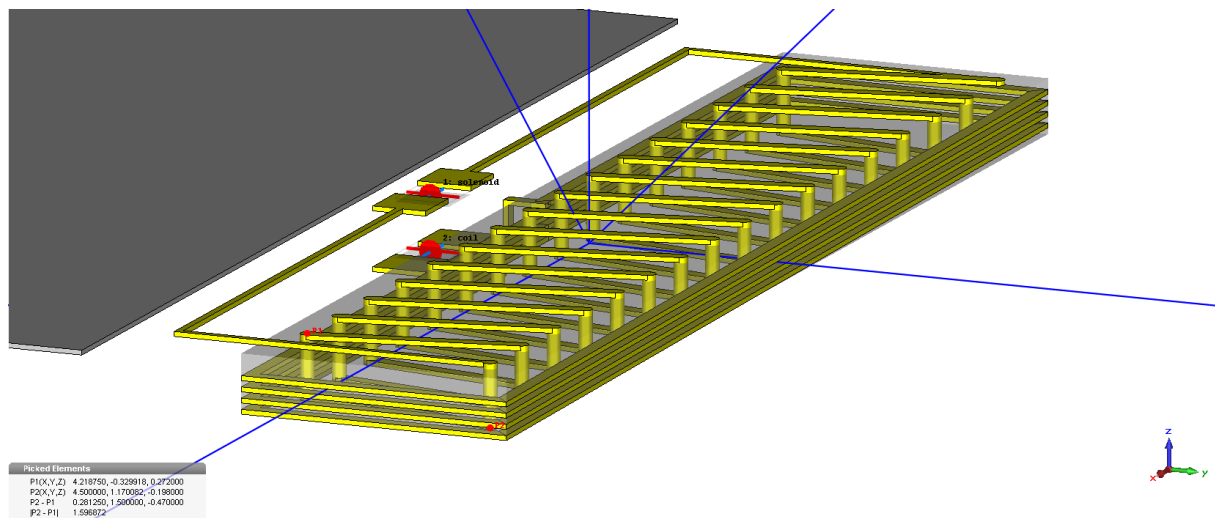


Figure 22: 3D detailed view of the hybrid coil

## 2.2.4 Comparison Between all Three Configurations

In this section a comparative analysis of the magnetic field generated by the 3 different coils in a  $\mu$ SD card will be presented.

The field will be evaluated along main directions defined in the previous section (H, V, D et al.) and will also be presented in a 2D plot of the magnetic field in the area surrounding the mobile device’s simplified model.

### 2.2.4.1 Magnetic Field Evaluation in Space and along Defined Directions

#### 2.2.4.1.1 2D Plot of Hz and Hx Field Components

In this section the field along the main path is presented. Dominant H-field components ( $H_z$ ,  $H_x$ ) are shown along paths V, D and H in Figure 23, Figure 24 and Figure 25, respectively.

From simulation results it is possible to note that the field generated by the solenoid and hybrid configuration is much higher than the one generated by the planar approach.

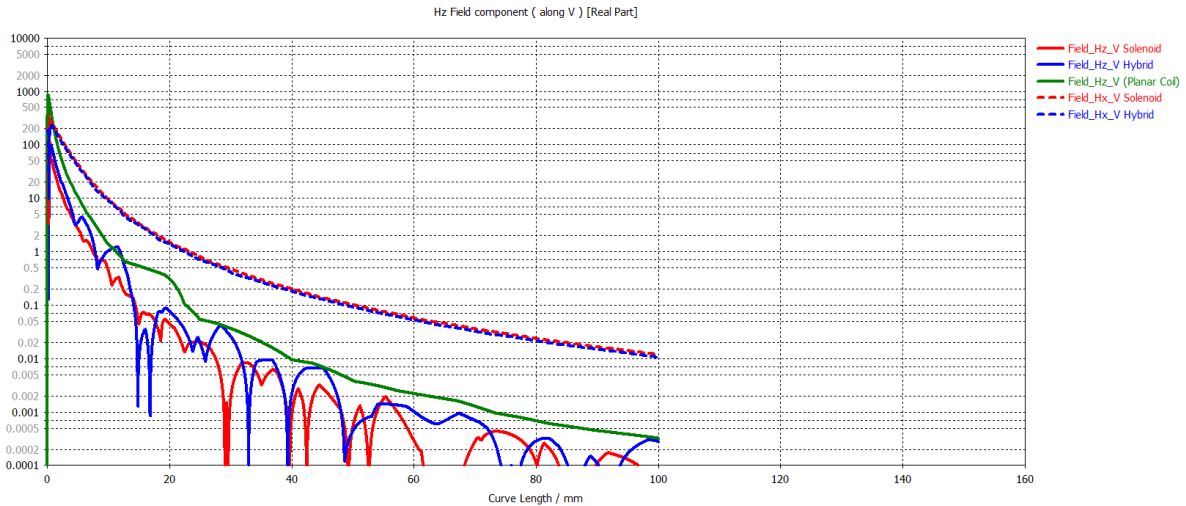


Figure 23: Hz field along V

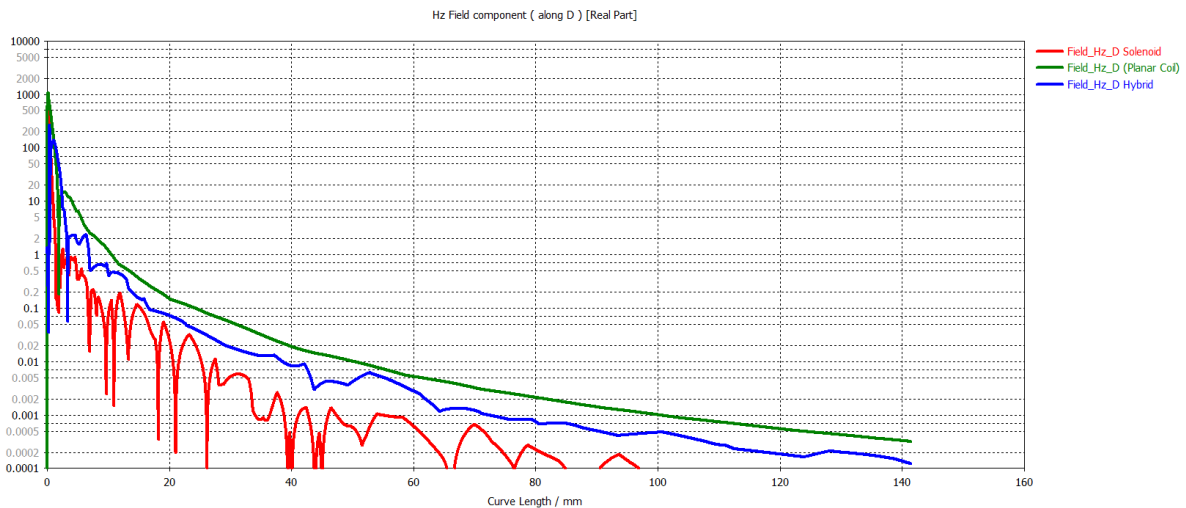


Figure 24: Hz field along D

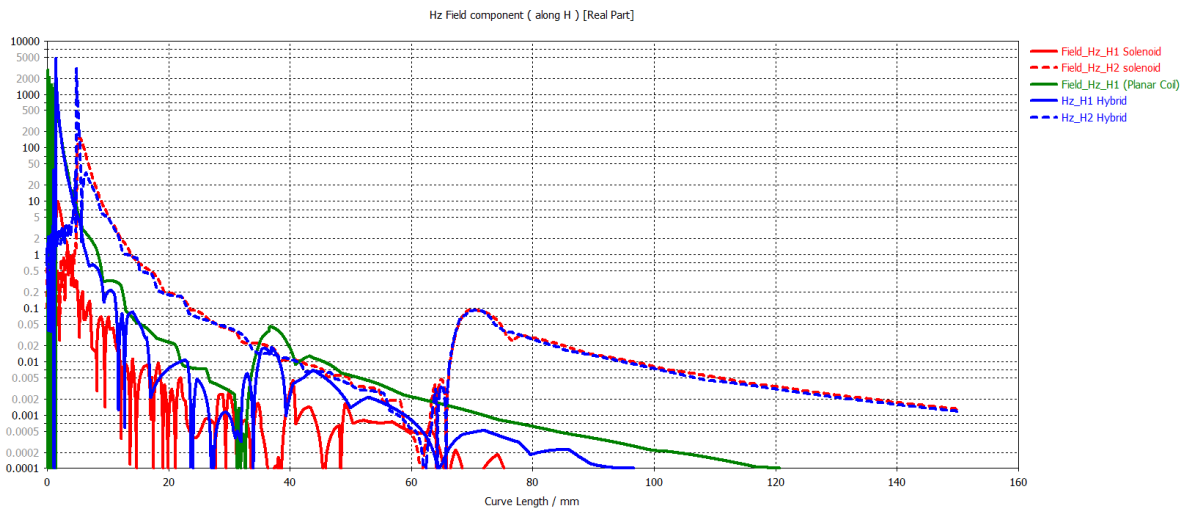


Figure 25: Hz field along H

#### 2.2.4.2 |H| Field Planar Plot

In the following section a 2D representation of the magnetic field in the area surrounding the mobile device model will be shown.

Each subsection will report the magnitude of magnetic field  $|H|$  and the magnitude of the separate components of the H field (  $|H_z|$ ,  $|H_y|$  and  $|H_x|$  ). In section 2.2.4.2.1 data related to the planar coil will be shown, sections 2.2.4.2.2 and 2.2.4.2.3 will report data related to solenoid and hybrid coils.

It can be observed that solenoid and hybrid coils present better distribution of the magnetic field in terms of covered area and strength of different components.



2.2.4.2.1 Planar Coil

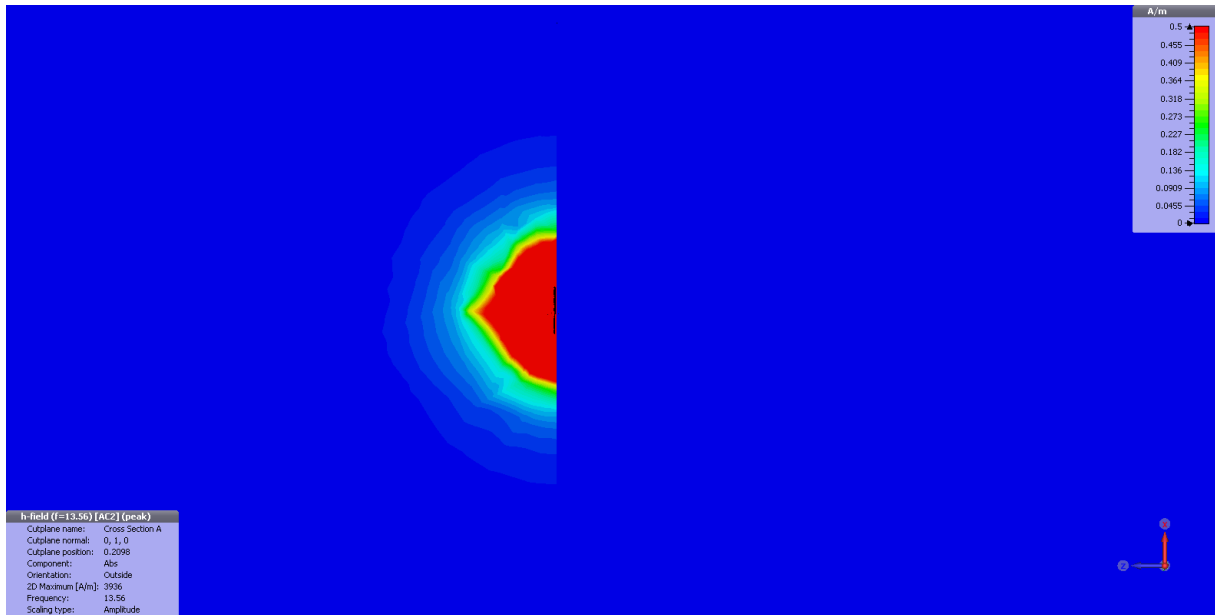


Figure 26: Planar coil |H| field distribution

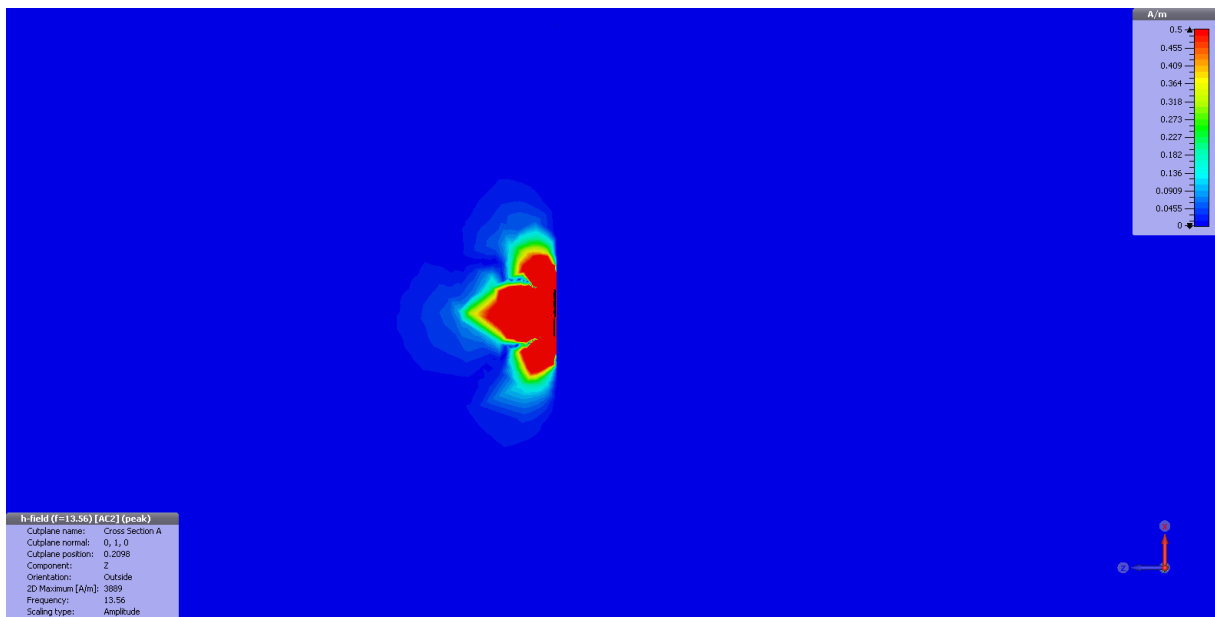


Figure 27: Planar coil |Hz| field distribution

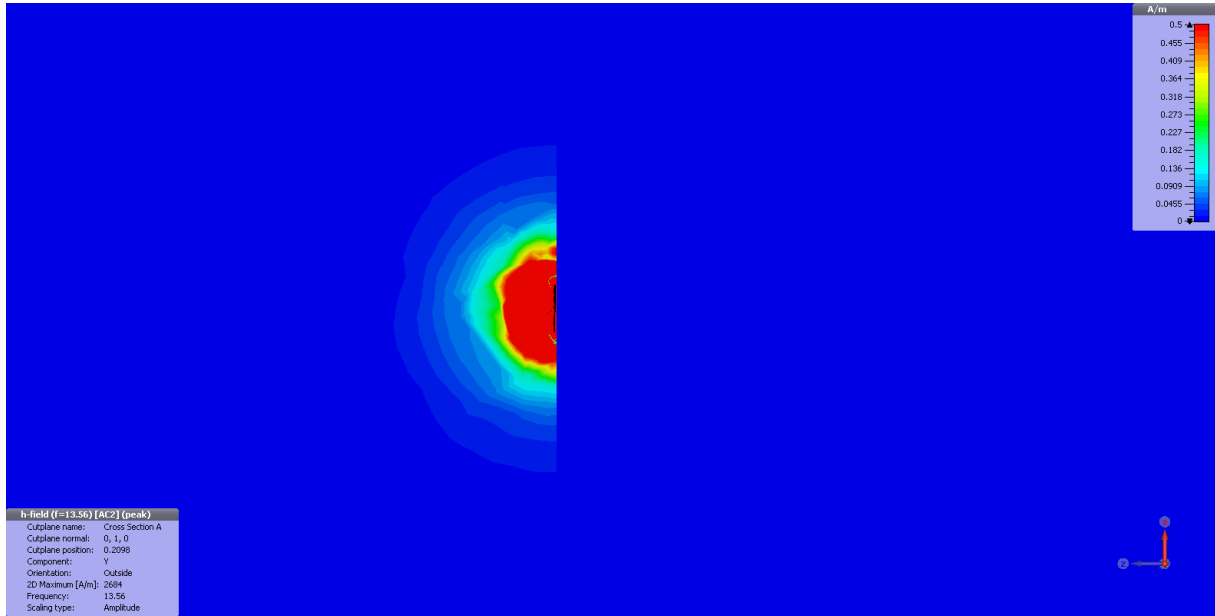


Figure 28: Planar coil  $|H_y|$  field distribution

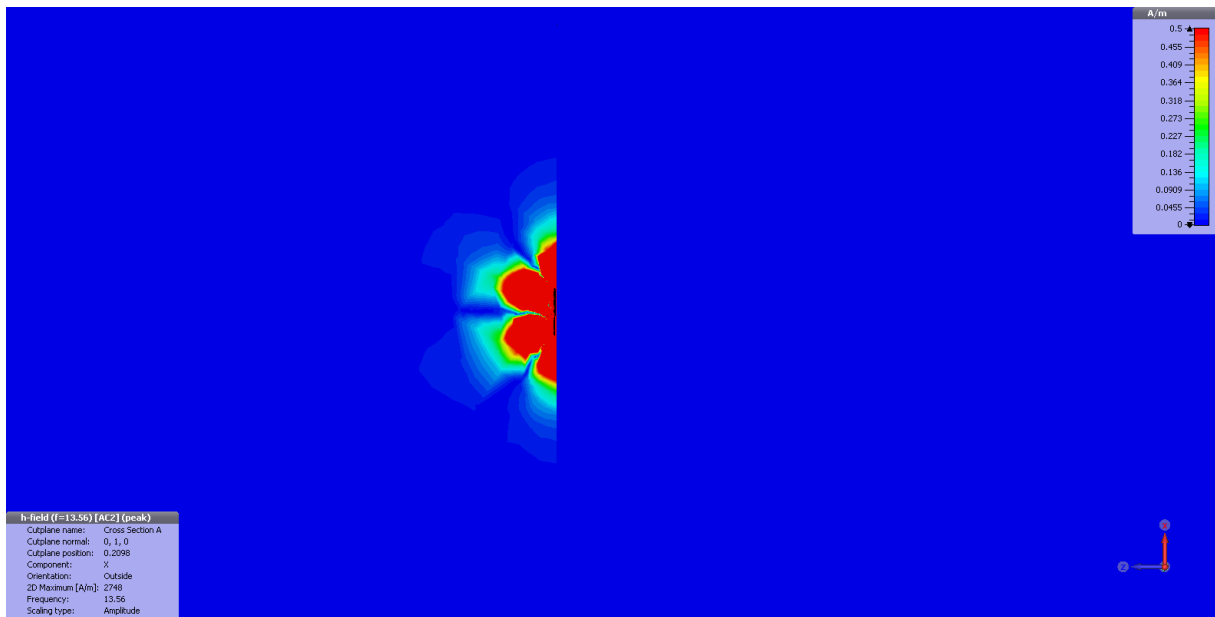


Figure 29: Planar coil  $|H_x|$  field distribution

2.2.4.2.2 Solenoid

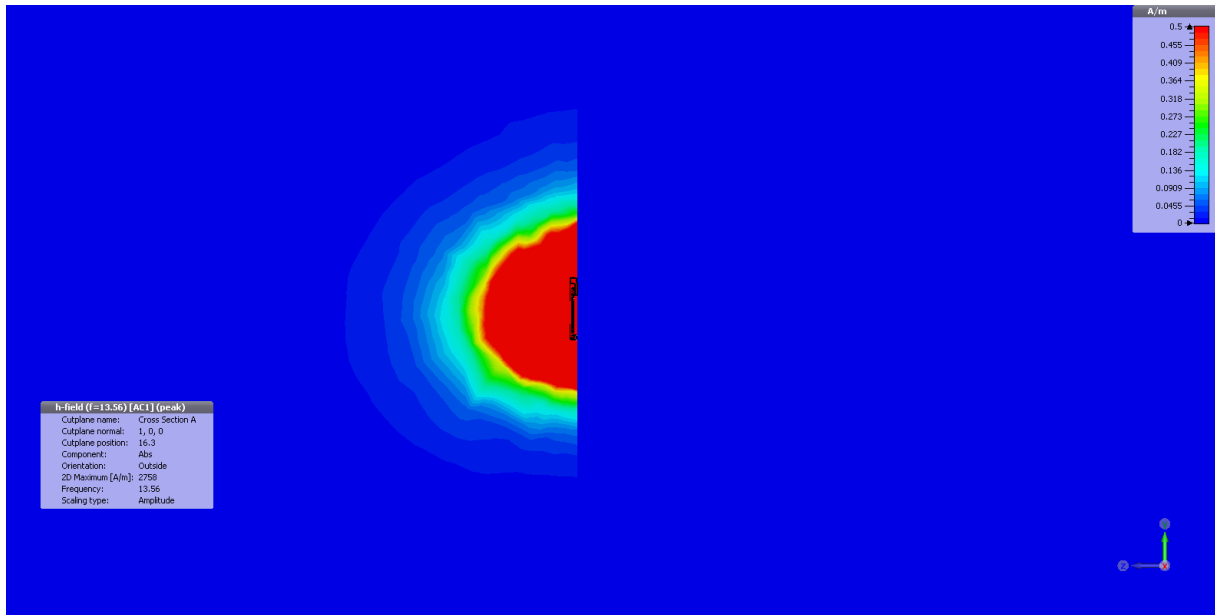


Figure 30: Solenoid |H| field distribution

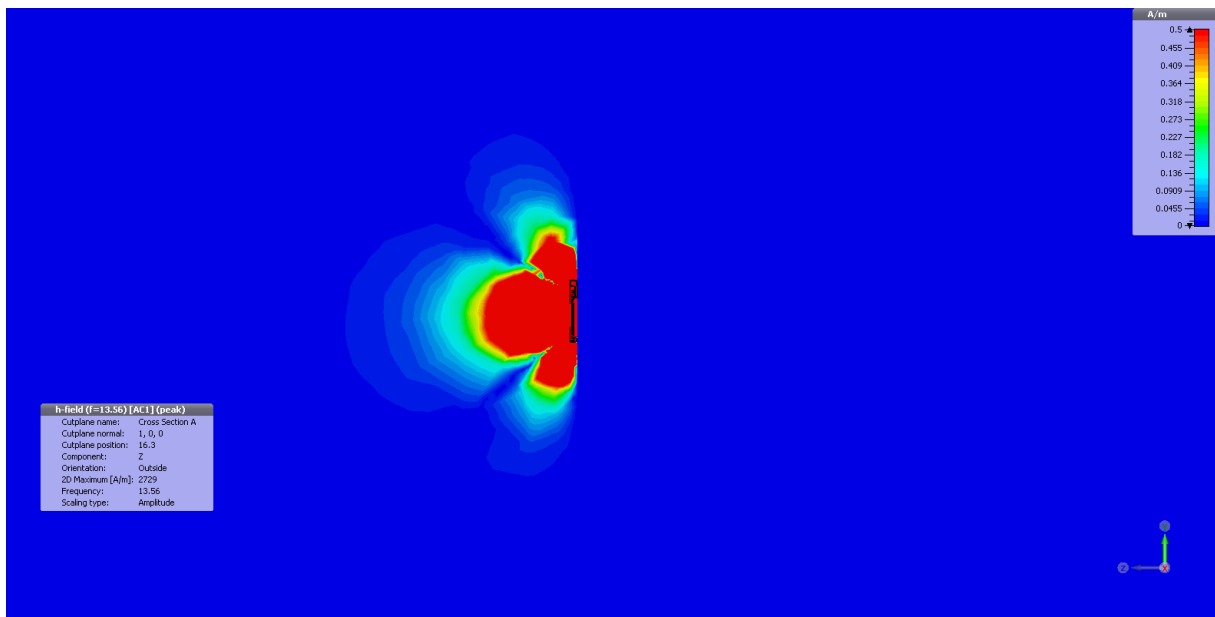


Figure 31: Solenoid |Hz| field distribution

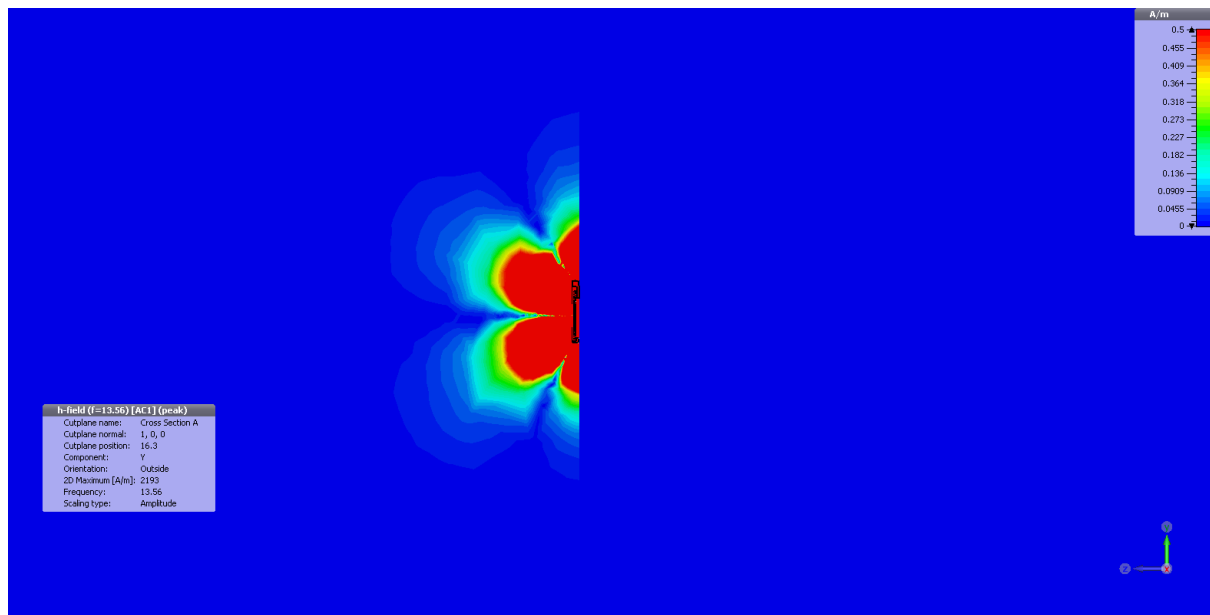


Figure 32: Solenoid  $|H_y|$  field distribution

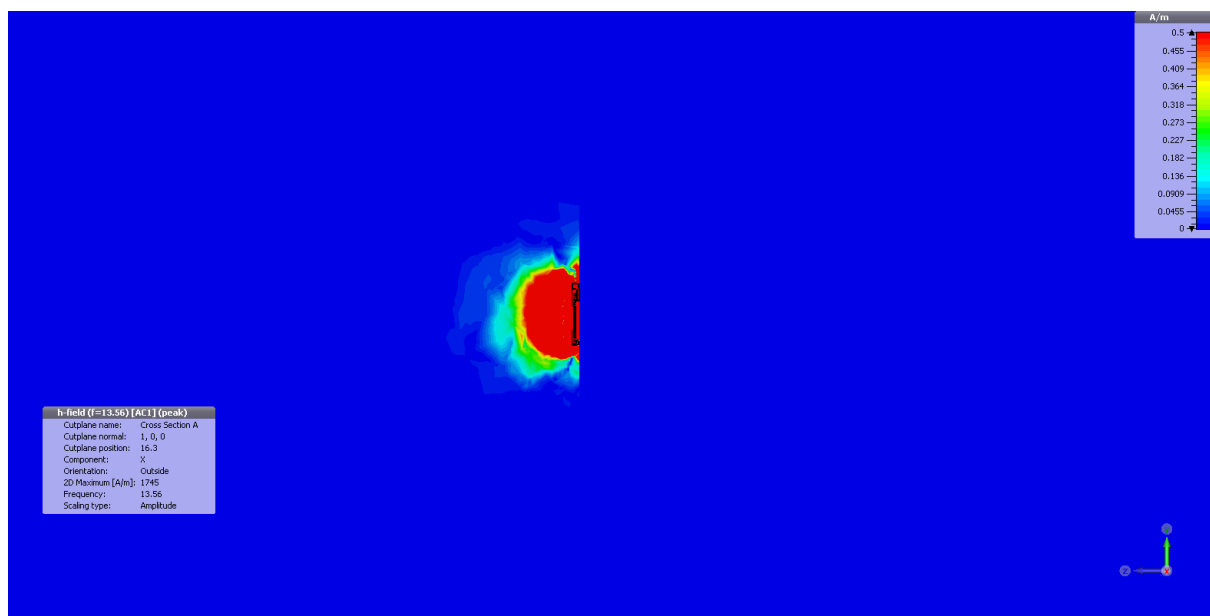


Figure 33: Solenoid  $|H_x|$  field distribution

### 2.2.4.2.3 Hybrid

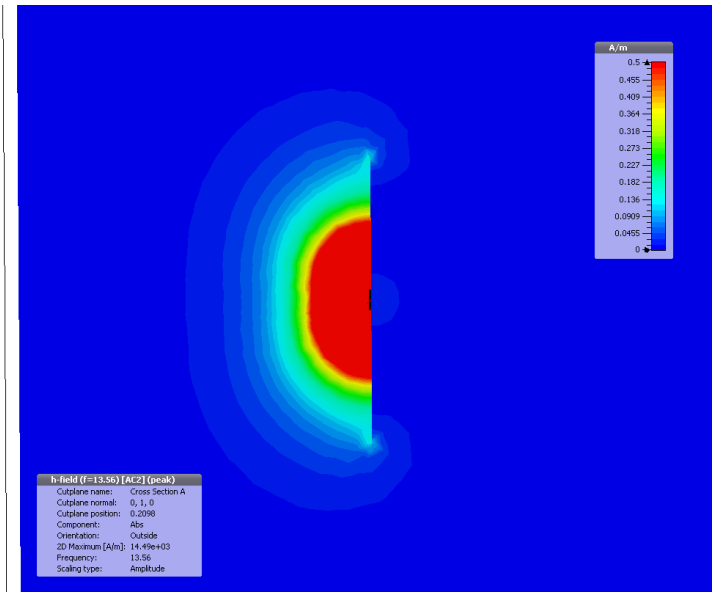


Figure 34: Hybrid |H| field distribution

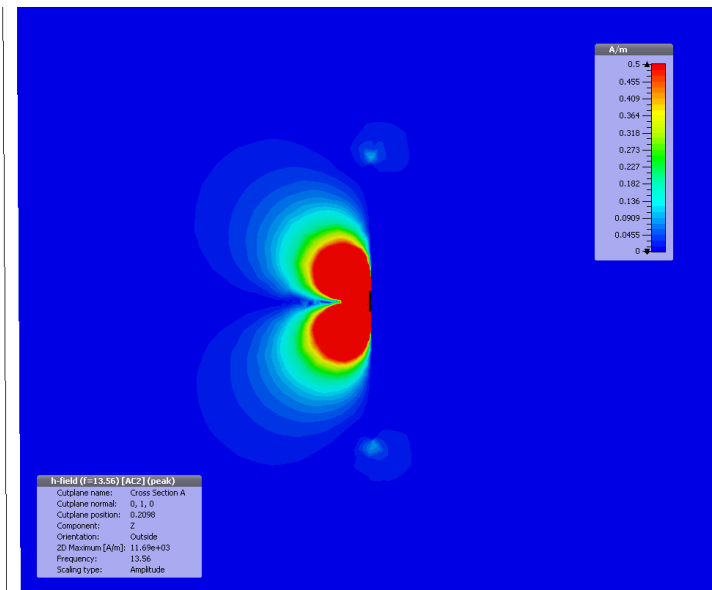


Figure 35: Hybrid |Hz| field distribution

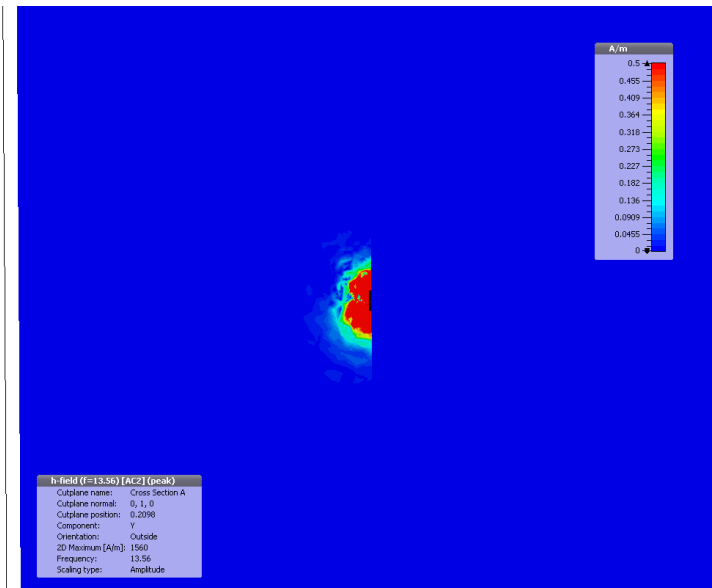


Figure 36: Hybrid |Hy| field distribution

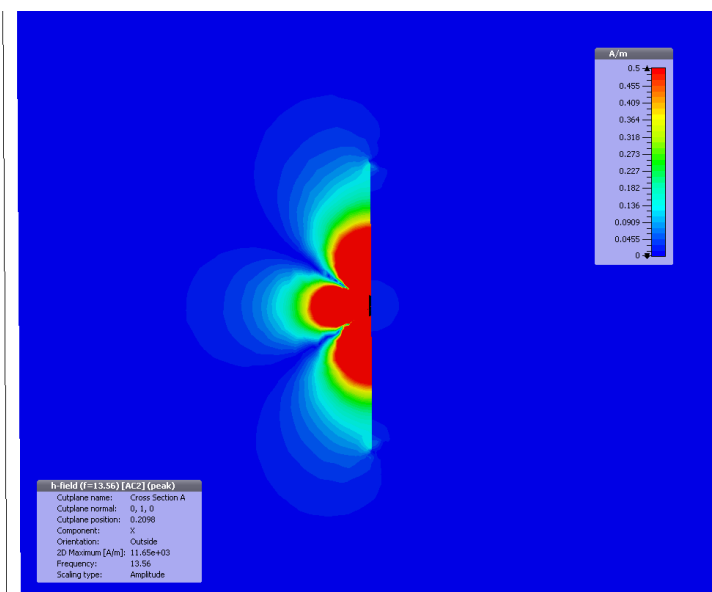


Figure 37: Hybrid |Hx| field distribution

## 2.3 nanoSIM Implementation

In this section simulations for the nanoSIM form factor will be presented. The finding of chapter 2.2 that solenoid and hybrid antenna have clear advantages over the planar approach will be taken into account by focusing on solenoid coils.

### 2.3.1 Antenna Concept

The nanoSIM implementation is based on a 2-step process. The antenna and ferrite are embedded in a stacked PCB structure with four metal layers. Booster chip, secure element and all other passive components are integrated in a cavity with standard wire bonding or by soldering.

From the antenna point of view, the closer the antenna is placed to the edge of the nanoSIM the better the performance. This is independent from the antenna type itself.

#### 2.3.1.1 nanoSIM Antenna Design

In most handsets the major part of the nanoSIM and therefore also a part the antenna is covered by the SIM socket. As explained in chapter 2.2 the solenoid antenna geometry guaranties the best performance for this environment. Furthermore the solenoid antenna has a symmetric radiation characteristic. That means it doesn't care if the contact pads of nanoSIM facing up or down, only the insertion direction has an influence on the operation.

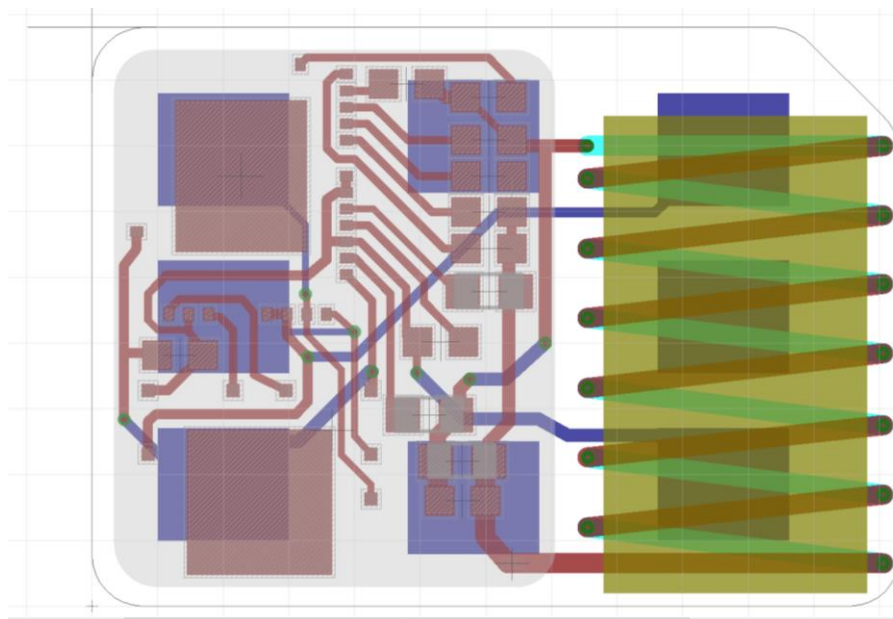


Figure 38: nanoSIM antenna design with ferrite core

## 2.3.2 Antenna Simulation

### 2.3.2.1 Equivalent Antenna Parameter EQV

Additional to the antenna geometries, the electrical parameters like inductance and quality factor are important for the antenna performance. The inductance of the antenna should be at least 300 nH to ensure an optimal reception performance. The quality factor (Q) of the antenna should be around 16. This value is a trade-off between signal strength and bandwidth. If the quality factor of the antenna is much higher, a resistor in series or in parallel can be used to lower the Q.

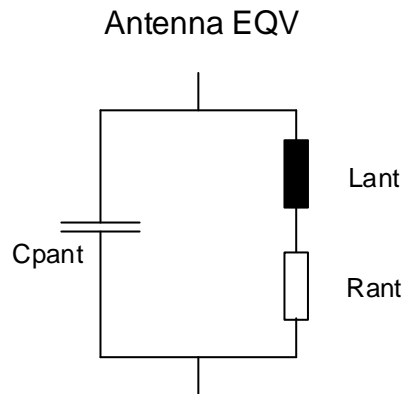


Figure 39: nanoSIM equivalent circuit of an antenna

Below are the simulation results of a 7-windings solenoid antenna in a free air environment. Simulation tool is ANSYS HFSS.

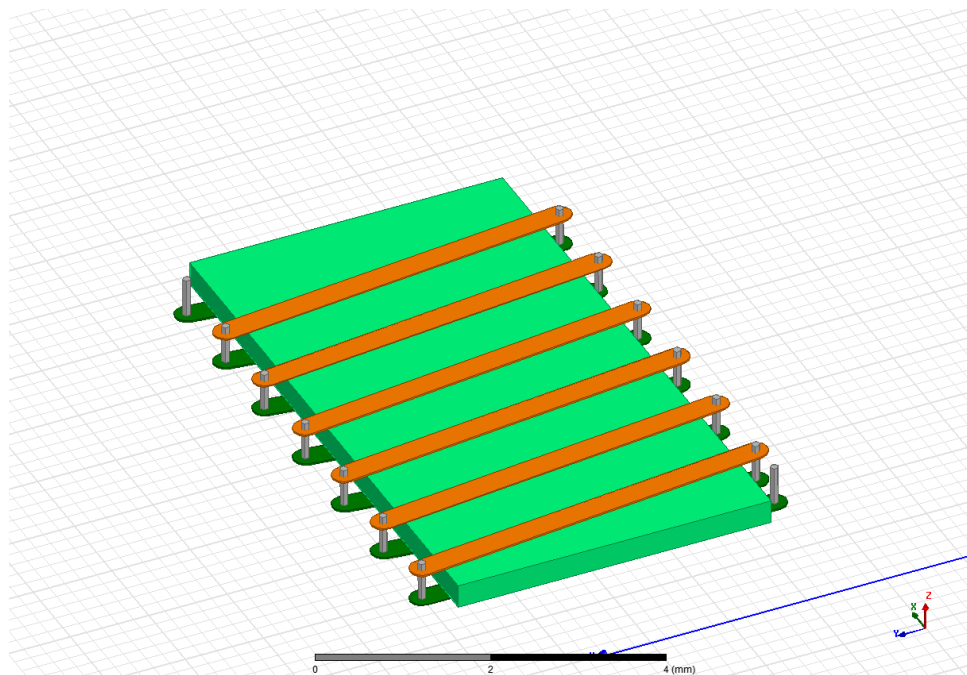


Figure 40: ANSYS HFSS EQV antenna simulation

EQV free air:

- $L = 312 \text{ nH}$
- $R = 0.7 \ \Omega$
- $Q = 37$



### 2.3.3 Antenna Matching

In order to operate highly efficient the antenna must be matched to the signal source. In the nanoSIM design the signal source is designed to drive a load of  $12 \Omega$ . An effective way to transform the impedance of the antenna to  $12 \Omega$  is shown in Figure 41.

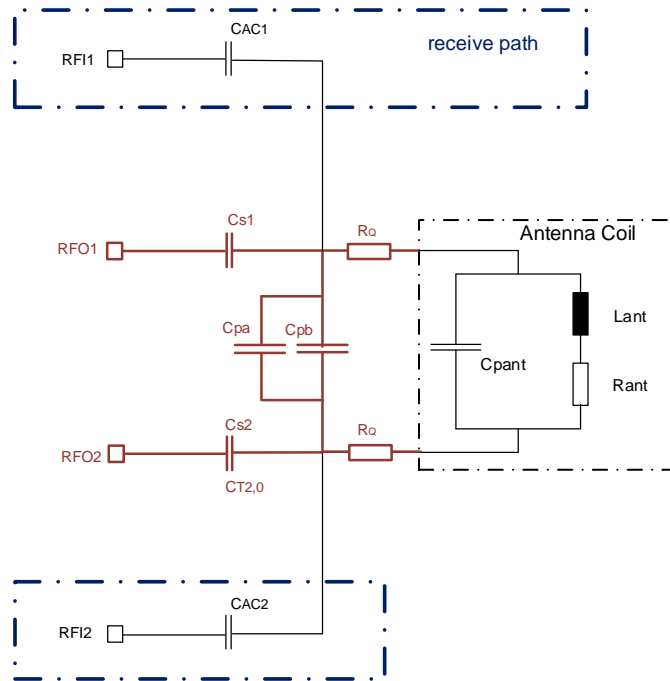


Figure 41: nanoSIM antenna matching circuit

The values of the matching components are based on the simulated EQV and expecting a minimum of detuning from the socket. The final nanoSIM will use the automatic antenna tuning of the AMS chip to operate at an optimal matching point. The automatic antenna tuning is based on a variable capacitor for  $C_{pant}$ . The Cap can be adjusted in a range from 200 pF to 650 pF. An antenna should have consequently an inductance of approximately of 350 nH.

Calculated values:

- $Cs1=Cs2= 470 \text{ pF}$
- $Cpa = 390 \text{ pF}$
- $Cpb = 0 \text{ pF}$
- $R_Q = 0.5 \Omega$
- $Q_{sys} \sim 13$

### 2.3.3.1 Simulation within Mobile Phone Model

Basis for the simulation is a model of a mobile phone. The communication performance is strongly dependent on the insertion direction of the nanoSIM. If the alignment of the nanoSIM dents inside the phone and the antenna is totally encapsulated by the socket, the signal generated by the antenna is extremely suppressed. The following simulation considers the antenna dents to the outside of the mobile.

Metal parts like aluminium case or a PCB with copper layer in close environment to the nanoSIM are disturbing the radiation. The most challenging simulation model for a nanoSIM design is made up of conductive material. In the simulation model the entire case is aluminium and only the gaps on the edge allowing the field running through.

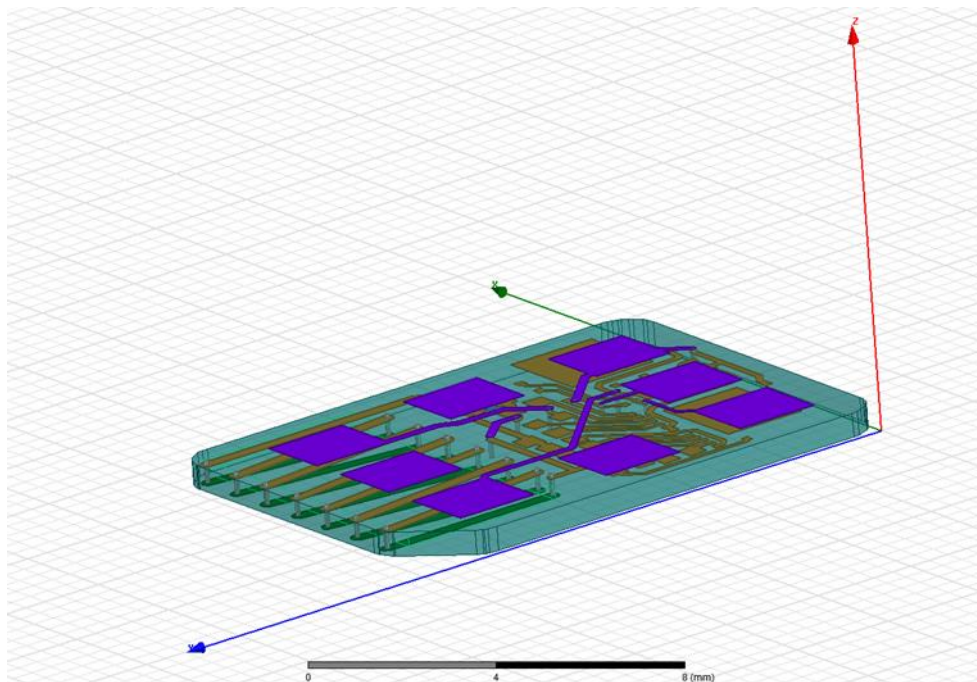


Figure 42: nanoSIM design with integrated antenna and contact pads

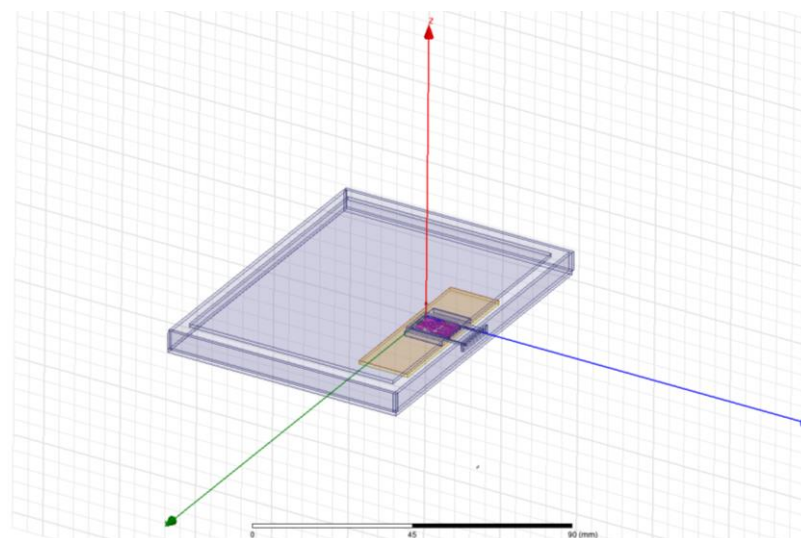


Figure 43: Simulation nanoSIM within mobile phone model

### 2.3.3.2 Radiated Field

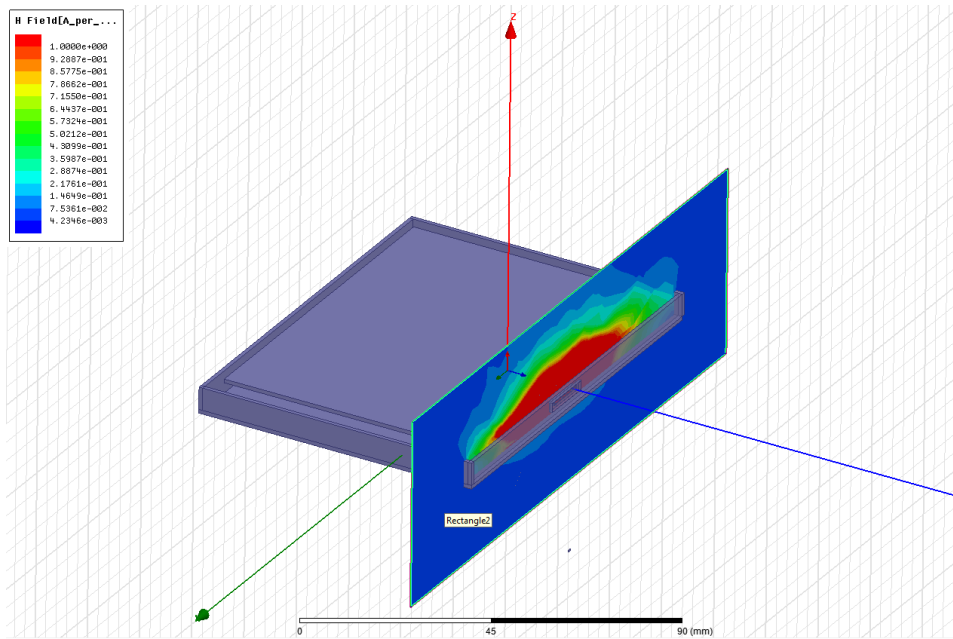


Figure 44: Field plot at the gap

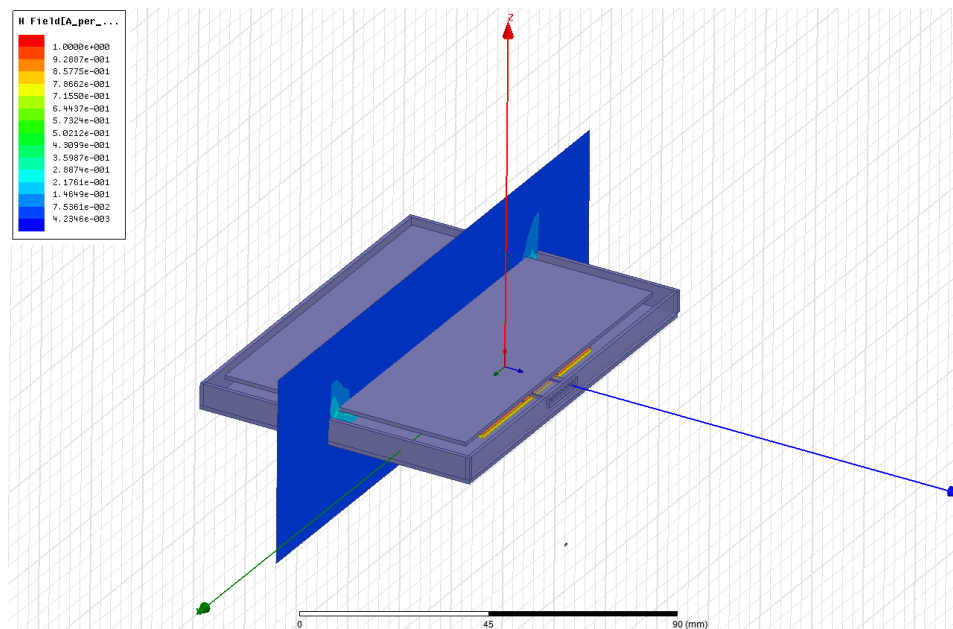


Figure 45: Field plot at the mid of the model

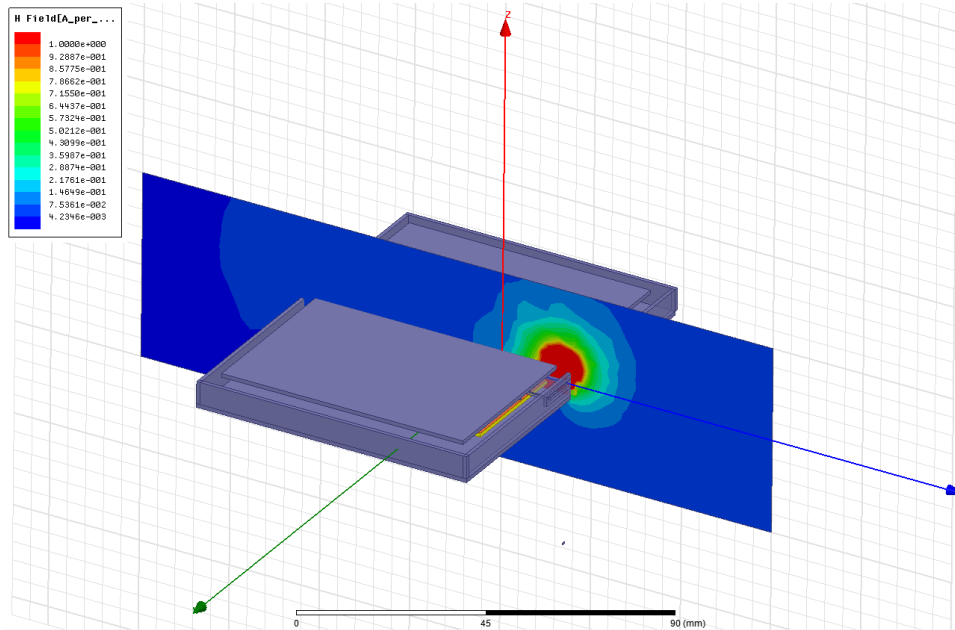


Figure 46: Field plot cross the model

### 2.3.4 Conclusion of nanoSIM Simulation

For the nanoSIM design it is a real challenge to operate in a phone with metal case. Additional to the disadvantage of the metal case also the current constraint for the SIM card limits the signal strength. Out of the simulation an operation seems to be possible. The effective performance will be seen with the demonstrator which is planned within WP5 "Integration, Prototyping".

## 2.4 Wearable Devices

During the project timeline, MATTHEW partners have identified new form factors that are likely to provide the same features and services introduced with the MATTHEW  $\mu$ SD and nanoSIM platforms. Especially a particular attention has been focused on wearable devices whose market is strongly growing. This new equipment appears as adequate candidate to propose to the end user secure applications like payment transactions, digital or physical access control, or transportation ticketing.

Furthermore, the connection with the user's mobile phone, usually established through a Bluetooth Low Energy interface, makes the embedded secure element 'visible' from the handset equipment and/or the cloud, if a data link is available. Therefore, it could be possible to exploit the secure capabilities of these wearable devices into the more complex multi-secure entities, in line with MATTHEW consortium targets (e.g. it could be possible, for example, to export security credentials from a SIM card, plugged into the user's mobile phone, to the secure element embedded into his connected bracelet).

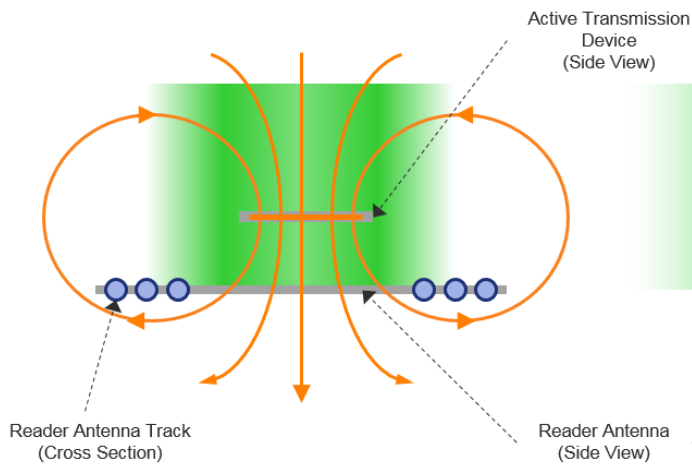
Finally, the active transmission technology, developed in the context of MATTHEW project, is particularly suitable for most connected bracelets and watches. Indeed, the level of hardware integration in such equipment is usually incompatible with common passive contactless technology that requires a pretty big antenna size in order to match the RF performance required by the contactless infrastructure. The active transmission technology offers, as introduced in previous chapters, the possibility to reduce significantly the antenna dimensions. Nevertheless, the design of magnetic antenna, in the context of wearable devices, is less restrictive compared to a  $\mu$ SD or a nanoSIM card:

- At the opposite of a memory card inserted into a 'pre-defined' location (and usually inappropriate for RF communication) inside a mobile equipment, the wearable device manufacturer will follow the design recommendations in order to achieve the best RF performance (i.e. no presence of metal close to the antenna coil; best location of the antenna coil to improve ergonomic; etc.).
- Even if the integration constraints are pretty strong, the size of the antenna coil inside a wearable device can be much larger ( $>1\text{cm}^2$ ) compared to the one embedded into a memory card ( $<40\text{mm}^2$ ).

In previous  $\mu$ SD and nanoSIM chapters, solenoid antennas appeared as the best topology to circumvent shielding effects of metal layers present above or below the card layout, thanks to their different magnetic field radiation scheme. Unlike mobile phone equipment, wearable devices offer a more permissive environment. In such condition a standard planar antenna will be appropriate to reach highest RF performances. Moreover, the use of other kinds of antenna geometries could affect significantly the user's experiences, who will tend to present his wearable equipment in front of a contactless terminal (worst case with a solenoid configuration that provides a different radiation scheme – refer to picture below).

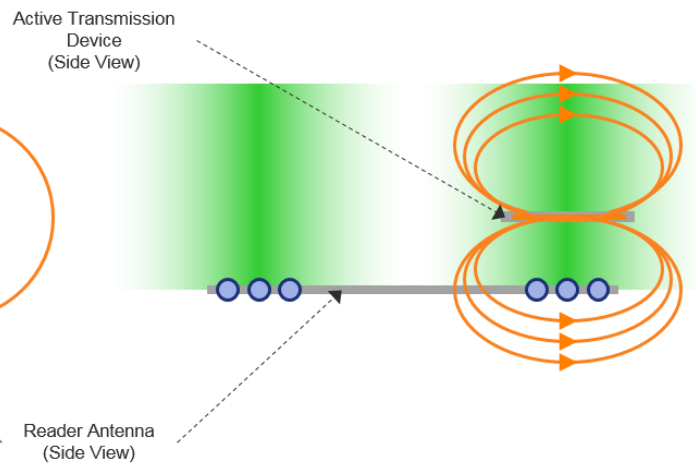
## Planar Antenna

Best performances obtained when active transmission device is presented above the reader antenna **area**



## Solenoid Antenna

Best performances obtained when active transmission device is presented above the reader antenna **tracks**.



In conclusion, standard magnetic planar antennas will be mainly deployed in wearable devices embedding the active transmission technology. The physical realization and final RF performance of such planar antennas don't appear to be a real challenge for the MATTHEW project and will not be investigated thoroughly in this document.

## Chapter 3 Load Modulation Simulation

One of the most critical aspects in tag design is to ensure that the tag will generate sufficient load modulation in order to be compliant with the specification defined by the standard.

To ensure that a certain level of Load Modulation (LMA) as defined in the “Report on use case and system architecture requirements” (deliverable D1.1), subsection 3.3.1.3 “3D RF Characteristics Requirements for transferable NFC components” is achieved, a simulation is needed.

State of the art in load modulation estimation is via measurements since it is very challenging to estimate the LMA via numerical calculation. However, in the next section we will present a new simulation approach that will allow an estimation of LMA via numerical calculation. The model will implement an ISO test bench, as defined in the ISO/IEC 10373-6 and ISO/IEC 14443-2:2012 for the calculation of LMA for CLASS 1 tag. (Note: Despite our antenna should be classified as passive Class 6, due to its small form factor; by taking advantage of the active transmission technology we will target a baseline performance comparable to a bigger class like Class1 tag).

### 3.1 Overview of ISO10373-6 Test Specification (for Passive Devices)

ISO 10373-6 specifies a special test set-up that shall be used to measure LMA and test functionality of passive tags and will in future integrate also a specification for active transmission technology based systems (at the moment the new standard with amendment for active systems is still under development and AMS, as well IFX and GTO are actively involved in the standardization process). The set-up of the electromechanical configuration is shown in Figure 47, Figure 48 and Figure 49.

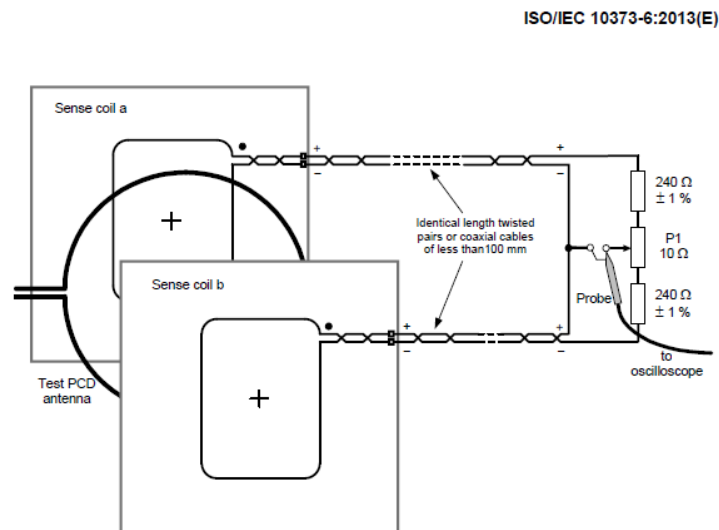


Figure 2 — Test set-up (principle)

Figure 47: ISO 10373-6 (test set-up view)

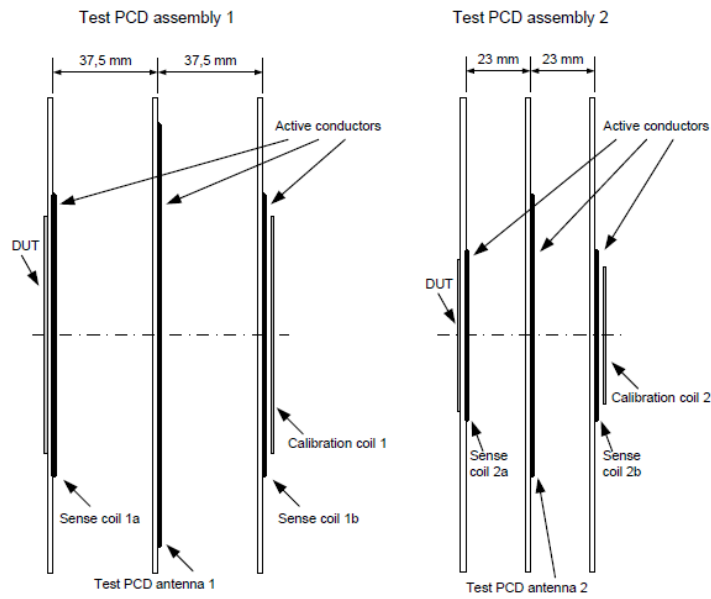


Figure 3 — Test PCD assembly 1 and test PCD assembly 2

Figure 48: ISO 10373-6 (test set-up view)

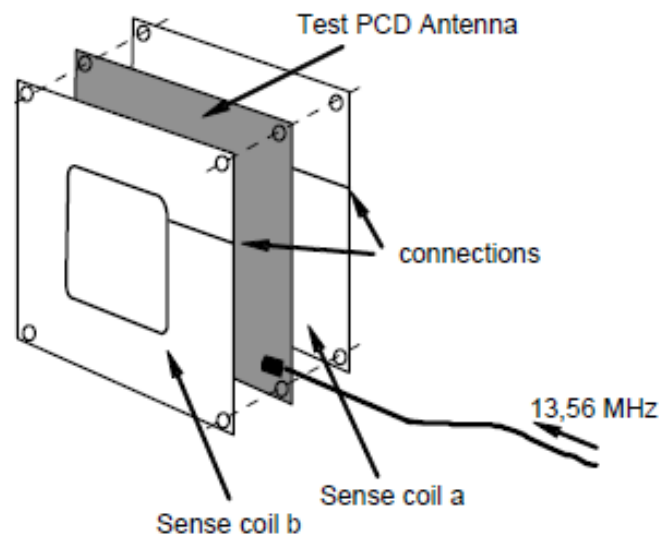


Figure C.3 — Sense coil assembly

Figure 49: ISO 10373-6 (test set-up view)



### 3.2 ISO 10373-6 Test Set-up Simulation Model (Class 1)

The above described ISO compliant test set-up defined for the verification of the LMA of any RFID tag (Class 1, 2 and 3) has been modelled in a 3D tool and simulated together with a  $\mu$ SD card with a solenoidal antenna in order to verify that the specified LMA can be achieved with a reasonable amount of current.

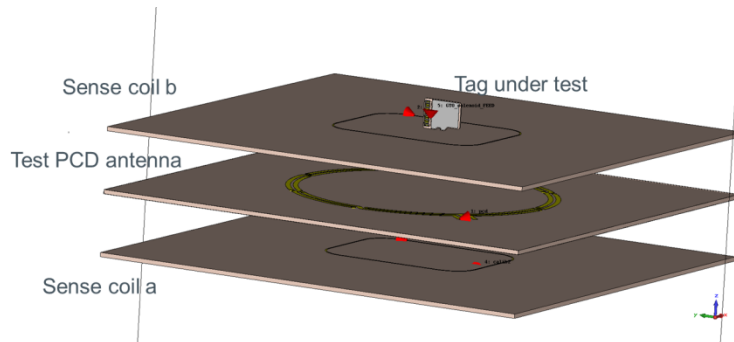


Figure 50: ISO 10373-6 (3D view simulation model)

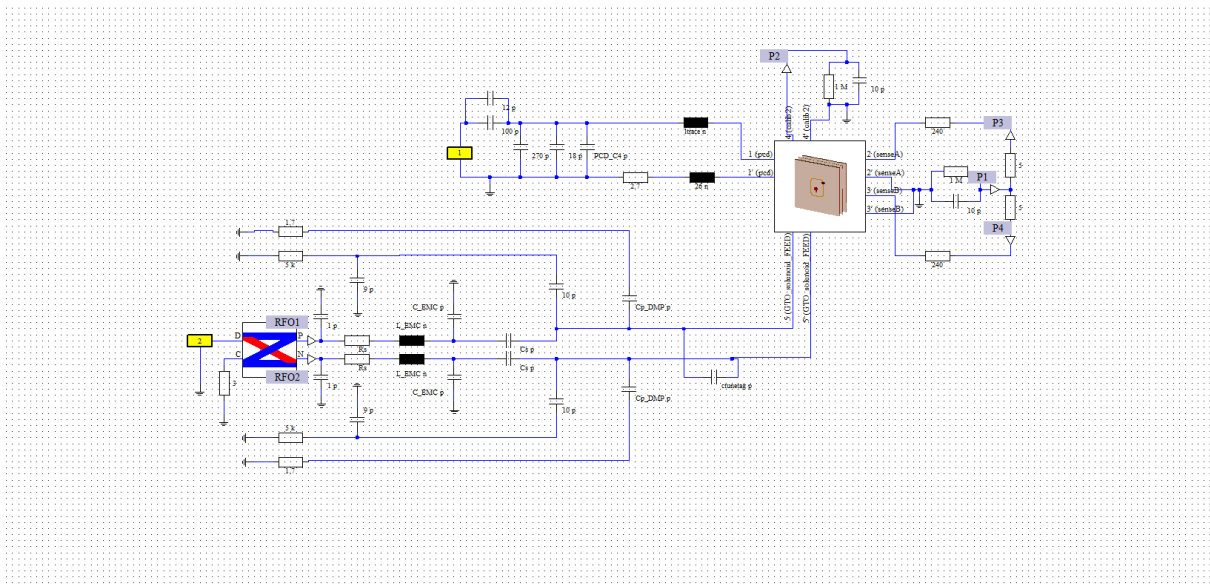


Figure 51: ISO 10373-6 (circuitual model used in co-simulation)

### 3.3 Simulation of Solenoid Coil

In this section an overview of the simulation results achieved by analysing a  $\mu$ SD card with a solenoid antenna will be shown. The simulation model emulates an active transmission technology based FE sending a well-defined bit stream, in phase with the PCD carrier signal, to the card coil and load modulation detected at the PCD is recorded and compared with the requirements defined in D1.1 (6mV load modulation).

The 3D electromagnetic model of the set-up used in the simulation is the one presented in Figure 50 and the circuitual model used to emulate the ISO test set-up functionality and record LMA is the one in Figure 51.

The driven voltage of the RF signal generated by the IC is shown in Figure 52. From Figure 52 it can be derived that the voltage is within the defined limit of 3V. Furthermore, the results shown in Figure 53 indicate that the current required by the system is approximately 250mA (confirming previous calculation) and as a last result we have a corresponding LMA level of  $\sim$ 7mV which perfectly fits to the target of an achievable 6mV LMA level (this corresponds to the maximal possible range).

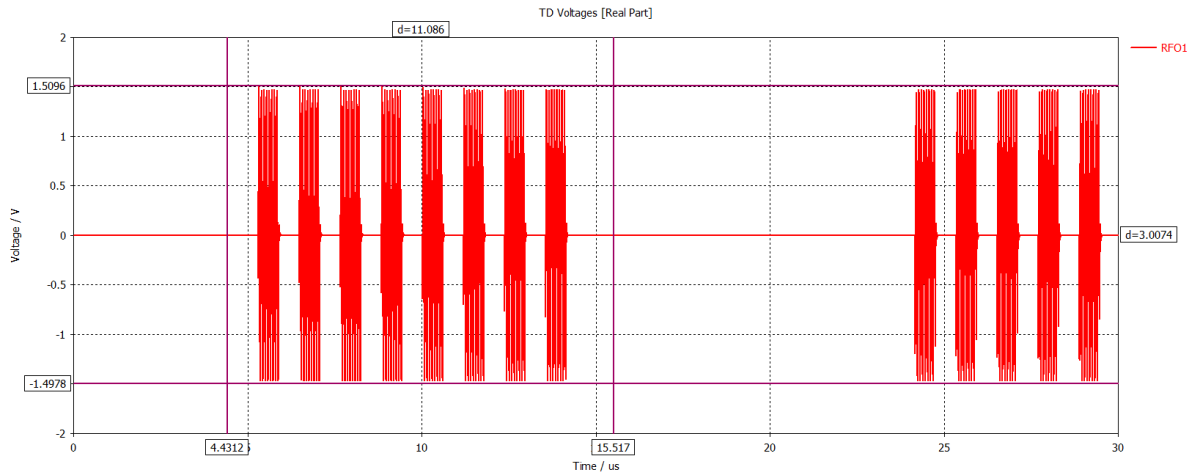


Figure 52: Output voltage at RFO pins of the IC

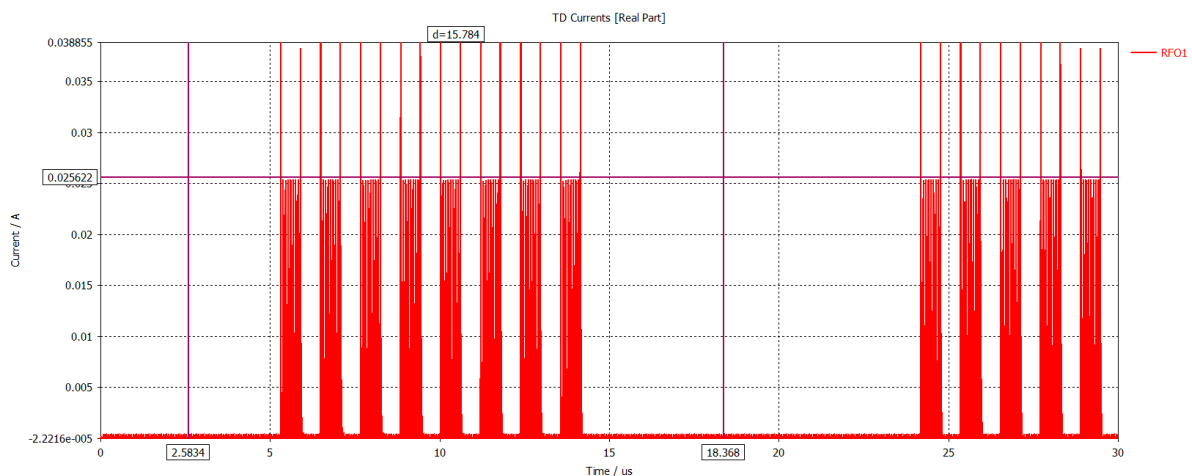


Figure 53: Output current at RFO pins of the IC

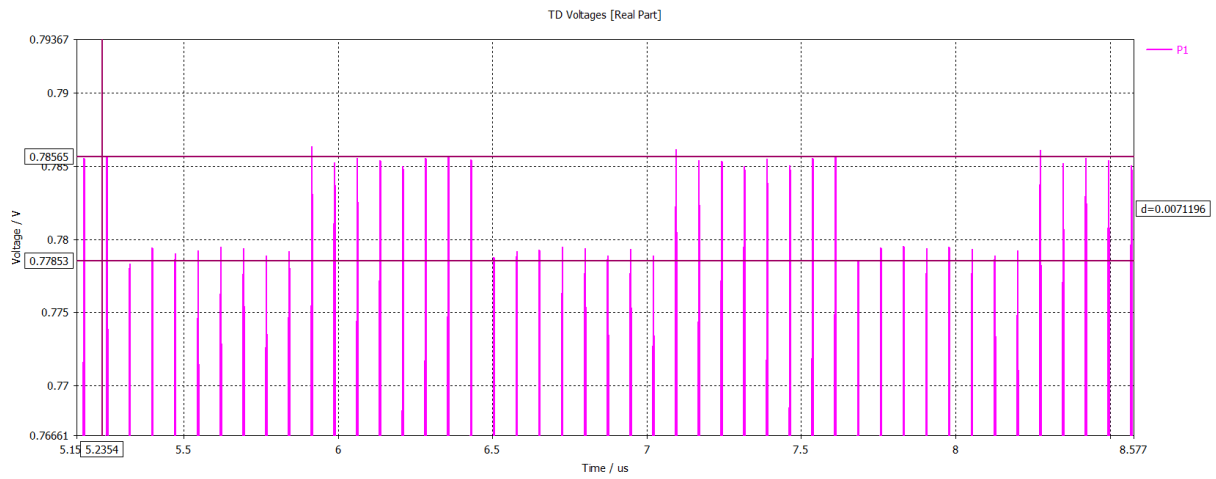


Figure 54: Achieved load modulation

## Chapter 4 Design Recommendations

In order to address possible EMC related issues, some basic design rules and recommendation have to be followed and applied in the system design.

### 4.1 RF Sub-System Block Diagram

In order to achieve efficiency in terms of radiated emission the RF sub-system has to be carefully designed implementing proper power supply decoupling by means of decoupling capacitors placed near to the RF IC, as well as implementing proper filtering and common mode rejection along the power supply line. An example of power supply filtering is shown in Figure 55

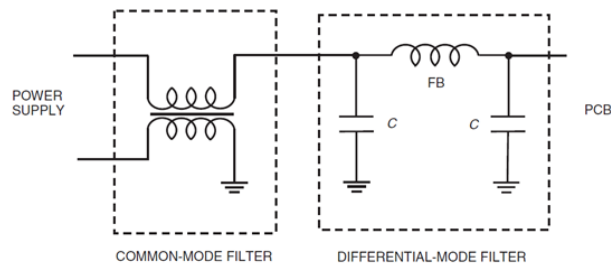


Figure 55: Power supply filtering

Once the power supply of the system is well decoupled and filtered it is very critical to define a proper low pass filter that allows to cut high harmonics of the signal generated by the active transmission technology based IC. In order to realize such filtering we recommend implementing a matching configuration that allows integration of a low pass structure having a cut of frequency in the range of 20MHz in order to suppress second and third harmonics of the 13.56MHz signal. The matching circuit must always be defined as in the block diagram shown in Figure 56 and reported in the following.

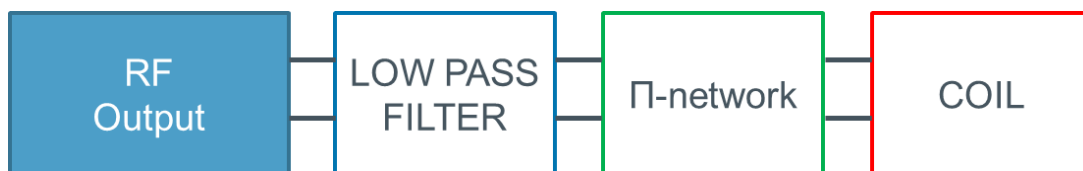


Figure 56: Matching block diagram

The above recommendations plus basic EMC mitigation technique rules in section 4.1.1 will lead to emission results compliant with FCC regulations. An example of measurement results (FCC) on test silicon (implementing active modulation transmission technique) is shown in section 4.2.

#### 4.1.1 EMC Mitigation Techniques

Here we summarize some general recommendations that need to be considered during PCB design in order to optimize EMC performance:

- Always consider and determine where and how the return currents are flowing.
- Partition mixed-signal PCBs with separate analog and digital sections.
- Do not split the current return plane; use one solid plane under both analog and digital sections of the board.
- Route digital signals only in the digital section of the board (for all digital related layers).
- Route analog signals only in the analog section of the board (for all analog related layers).
- In case ground or power planes are split for a specific reason (i.e. mechanical and or electrical), please do not run any traces across the split on an adjacent layer.
- Traces (analog or digital) that must go over a power plane split must be on a layer adjacent to a solid ground plane (analog or digital)
- A/D and D/A converters, as well as most other mixed-signal ICs, should be considered as analog devices with a digital section, not as digital devices with an analog section.
- The designation AGND and DGND on the pins of a mixed signal IC refers to where the pins are connected internally, and it does not imply where or how they should be connected externally. On most mixed-signal ICs, both the AGND and DGND pins should be connected to the analog return plane.
- The digital decoupling capacitor should be connected directly to the digital ground pin.
- The decoupling capacitors are needed to supply, through a low-inductance path, some or all of the transient power supply current required when an IC logic gate switches.
- Decoupling capacitors are needed to short out, or at least reduce, the noise injected back into the power ground system.
- Decoupling is not the process of placing a capacitor adjacent to an IC to supply the transient switching current; rather is it the process of placing an L–C network adjacent to the IC to supply the transient switching current.
- The value of the decoupling capacitor(s) is important for the low-frequency decoupling effectiveness.
- The value of the decoupling capacitor(s) is not important at high frequencies.
- At high frequencies the most important criteria is to reduce the inductance in series with the decoupling capacitors.
- Effective high-frequency decoupling requires the use of a large number of capacitors.
- In most cases, the use of single value decoupling capacitors performs better than multiple capacitors of different values.
- For optimum high-frequency decoupling, discrete capacitors should not be used at all; rather, a distributed capacitor PCB structure should be used.
- The number one rule of decoupling is to have the current flow through the smallest loop possible.

## 4.2 Example of a Test System (Emission Measurement)

Here below a picture of a test system (active transmission technology test silicon) on a mobile device and emission data is shown.

Due to confidentiality of the picture below no more details will be given.

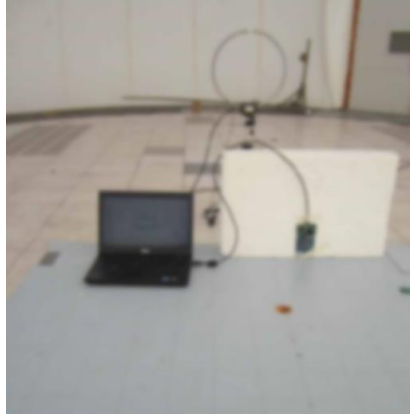


Figure 57: Mobile device in semi-anechoic chamber

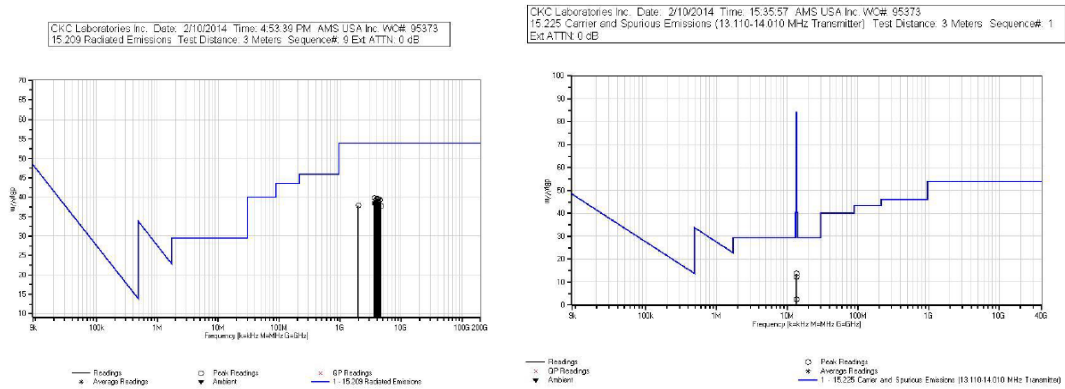


Figure 58: Radiated emission (black dot)

## Chapter 5 Conclusion

The analysis of different antenna types clearly showed the advantage of “solenoidal” based antennas in mobile applications due to their reduced interaction with metal parts surrounding the antenna and their ability to generate a magnetic field that shall enhance user experience and system functionality. The study also showed that with proper matching configuration the amount of consumed power can be limited and current can be controlled in order to be within a well-defined range.

Selected antenna concepts have been compared regarding the ability to generate a sufficient level of LMA by mean of 3D electromagnetic simulations, a possible hardware implementation in a nanoSIM format has been investigated and a flexible implementation based on the so-called “Chip on Board” approach has been selected as the most suitable for the prototyping of the final demonstrator.

Final validation of numerical and theoretical results will be done in WP5 and WP6 when silicon and demonstrator will be available and tested according to the ISO 10373-6.

## Chapter 6 List of Abbreviations

ALM	Active Load Modulation
COB	Chip on Board
EMC	Electromagnetic Compatibility
EQV	Equivalent Circuit
FCC	Federal Communications Commission
FE	Frontend
IC	Integrated Circuit
ISO	International Organization for Standardization
LMA	Load Modulation
NFC	Near Field Communication
PCB	Printed Circuit Board
PCD	Proximity Coupling Device
PTH	Plated-Through Holes
Q	Quality Factor
RF	Radio Frequency
RFID	Radio Frequency Identification
SIM	Subscriber Identification Module
SD	Secure Digital